Cell. Mol. Life Sci. (2016) 73:2661–2679
DOI 10.1007/s00018-016-2244-8

Cellular and Molecular Life Sciences

MULTI-AUTHOR REVIEW

GH13 amylosucrases and GH70 branching sucrases, atypical enzymes in their respective families

Claire Moulis[1,2,3] · **Isabelle André**[1,2,3] · **Magali Remaud-Simeon**[1,2,3]

Received: 21 April 2016 / Accepted: 22 April 2016 / Published online: 3 May 2016

Abstract Amylosucrases and branching sucrases are α-retaining transglucosylases found in the glycoside-hydrolase families 13 and 70, respectively, of the clan GH-H. These enzymes display unique activities in their respective families. Using sucrose as substrate and without mediation of nucleotide-activated sugars, amylosucrase catalyzes the formation of an α-(1 → 4) linked glucan that resembles amylose. In contrast, the recently discovered branching sucrases are unable to catalyze polymerization of glucosyl units as they are rather specific for dextran branching through α-(1 → 2) or α-(1 → 3) branching linkages depending on the enzyme regiospecificity. In addition, GH13 amylosucrases and GH70 branching sucrases are naturally promiscuous and can glucosylate different types of acceptor molecules including sugars, polyols, or flavonoids. Amylosucrases have been the most investigated glucansucrases, in particular to control product profiles or to successfully develop tailored α-transglucosylases able to glucosylate various molecules of interest, for example, chemically protected carbohydrates that are planned to enter in chemoenzymatic pathways. The structural traits of these atypical enzymes will be described and compared, and an overview of the potential of natural or engineered enzymes for glycodiversification and chemoenzymatic synthesis will be highlighted.

✉ Magali Remaud-Simeon
remaud@insa-toulouse.fr

[1] Université de Toulouse, INSA, UPS, INP, LISBP, 135 Avenue de Rangueil, 31077 Toulouse, France

[2] CNRS, UMR5504, 31400 Toulouse, France

[3] INRA, UMR792 Ingénierie des Systèmes Biologiques et des Procédés, 31400 Toulouse, France

Keywords Sucrose-active enzymes · Amylosucrase · Branching sucrase glucansucrase · Transglucosylation

Abbreviations

CD	Catalytic domain
DSR	Dextransucrase
GBD	Glucan binding domain
GH	Glycoside hydrolase
GS	Glucansucrase
MTH	Maltooligosyltrehalohydrolase
MTS	Maltooligosyltrehalose synthase

Introduction

Compared with most glycoside-hydrolases, glucansucrases (GSs) are naturally very efficient α-transglucosylases. From sucrose substrate, they catalyze α-glucan synthesis with the concomitant release of fructose. Linear and branched polymers can be formed, which can vary in terms of type of glucosidic linkages as well as degree and spatial arrangements of branches [1, 2]. These α-retaining enzymes are found in the clan GH-H of the CAZy classification of glycoside-hydrolases, where amylosucrases belonging to GH13 family synthesize an amylose-like polymer and can be distinguished from GH70 glucansucrases, which display wider linkage specificities [3, 4]. In particular, GH70 dextransucrases catalyze the formation of dextrans, polymers mainly composed of α-1,6 linked glucosyl units in their linear chain and harboring various types of α-(1 → 2), α-(1 → 3), or α-(1 → 4) linked branches. Over the past years, these transglucosylases have emerged as valued tools to synthesize well-defined carbohydrate-based structures [5, 6]. Not only do these enzymes use as

substrate an abundant agroresource, sucrose, but they also share a remarkable versatility regarding acceptor substrate. With the increasing and continuous flux of novel sequences, data mining has opened the way to the discovery of new activities, in particular novel enzymes of GH70 family specialized in dextran branching. In this review, the focus will be placed on GH13 amylosucrases and GH70 dextran branching sucrases. These enzymes stand apart in their respective families. Their particularity in terms of specificity, mechanism, and structure–activity relationships will be described. Insight will be provided on their natural aptitude for synthesizing novel carbohydrate-based structures. Particular attention will be finally given to protein engineering strategies that were recently applied to these catalysts and considerably enlarged the repertoire of accessible reactions.

GH13 amylosucrases and GH70 dextran branching sucrases

Atypicity of amylosucrases in GH13 family

Amylosucrase activity was first described in 1946 by Hehre and Hamilton, who identified in the culture supernatant of *Neisseria perflava* the presence of an activity responsible for the synthesis of an amylose-like polymer, in the absence of any nucleotide-activated sugars [7–9]. Then, other intracellular amylosucrase activities were identified in various species of *Neisseria* (*N. canis, N. cinerea, N. dentrificans, N. sicca,* and *N. subflava* [10]). These bacteria belong to the microbiota of the buccal cavity and may be potentially involved in the formation of dental carries [11, 12]. In 1983, the strain *Neisseria polysaccharea* was isolated from the throat of healthy children [13] as a producer of extracellular amylosucrase. The gene encoding this enzyme was cloned in fusion with a GST encoding tag and sequenced [14], and the recombinant enzyme was biochemically characterized [15]. The amylosucrase sequence revealed that it belongs to the α-amylase superfamily (GH13 family), in which it is, however, the sole enzyme that catalyzes the formation of an amylose-like polymer from sucrose alone. Recently, production systems of recombinant *N. polysaccharea* amylosucrase in fusion with His tag were also reported, and it was shown that these purification tags do not impair the enzyme catalytic properties [16]. Since 2005, several recombinant amylosucrases from *Deinococcus radiodurans* [17], *Deinococcus geothermalis* [18], *Deinococcus radiopugnans* [19], *Arthrobacter chlorophenolicus* [20], *Alteromonas macleodii* [21], *Methylobacillus flagellatus* [22], cyanobacterium *Synechococcus* sp. [23], and thehalotolerant methanotroph *Methylomicrobium alcaliphilum* 20Z [24] have been described, revealing that these enzymes are much more widespread than previously thought. Among them, the amylosucrase from *N. polysaccharea* (*Np*As) remains the most investigated so far in the literature.

The physiological role of amylosucrases has not been extensively studied yet. Buttcher et al. proposed that its polymer product might protect the cell [25]. As *N. polysaccharea* amylosucrase is very efficient for elongating glycogen branches, it was suggested that the enzyme could be involved in energy storage [26, 27]. More recently, Perez-Cenci et al. proposed that the amylosucrase from the cyanobacterium *Synechococcus* sp PCC 7002 could play a role in sucrose catabolism [23]. In this species, the amylosucrase encoding gene (*ams*A) was co-expressed with three other genes (*spp*A, *sps*A, and *frk*A), forming the Suc cluster. *SppA* and *spsA* encode a sucrose-phosphate phosphatase and a sucrose-phosphate synthase, respectively, and would be responsible for sucrose synthesis, whereas *amsA* and *frkA* (encoding an amylosucrase and a fructokinase) would be involved in sucrose catabolism to yield maltooligosaccharides and fructose-6P. These results suggest that, in cyanobacteria, amylosucrase participates in energy storage from sucrose. Investigations on sucrose metabolism in the halotolerant model methanotroph *Methylomicrobium alcaliphilum 20Z* highlighted the presence of an operon encoding sucrose synthesizing enzymes (sucrose-phosphate synthase and sucrose-phosphate phosphatase) and utilizing enzymes (fructokinase and amylosucrase) [24]. In such halotolerant organisms, intracellular sucrose accumulation is often one of the responses to low water activity [28], which led the authors to suggest that the main function of this operon might be de novo sucrose synthesis. Being involved in dissipation of energy excess through glycogen elongation, amylosucrase would participate in a "sucrose cycle" that could balance the internal concentration of sucrose. Amylosucrase-like sequences were revealed in 53 bacterial species, including 21 Proteobacteria, 18 Cyanobacteria, but no Firmicutes. Analogous gene clusters were identified in various Proteobacteria, showing that such "sucrose cycles" involving amylosucrase activity are probably widespread [24].

Discovery of dextran branching sucrases

The first GH70 glucansucrase was discovered in sucrose-broth cultures of *Leuconostoc mesenteroides* lactic acid bacteria [29]. The enzyme was shown to synthesize a water-soluble dextran [α-(1 → 6) linked D-glucan] from sucrose only, without any mediation of nucleotide-activated sugars unlike most of the polysaccharide-synthesizing enzymes. Dextran from *L. mesenteroides* sp. was the first microbial polysaccharide to be commercialized for use as blood plasma substitute during the Second

World War. With the view of finding alternative producers of clinical dextrans, Jeanes et al. produced and characterized 96 glucans synthesized by lactic acid bacteria grown on sucrose as carbon source [30]. This pioneering study shed light on the remarkable diversity existing in glucans produced by these species. In particular, one strain—*L. mesenteroides* NRRL B-1299 (today reclassified as *Leuconostoc citreum*)—produces a branched dextran, later characterized with a high degree of α-(1 → 2) branching linkages [30, 31]. The complex structure of the polymer was extensively studied. Notably, all the dextran fractions isolated from the fermentation broth contained a high percentage of α-(1 → 2) linkages (up to 30 %) and a few α-(1 → 3) linkages [32–34]. The physiological role of this dextran was never investigated in detail. When grown on sucrose, *L. citreum* NRRL B-1299 cells are surrounded by a shell of insoluble dextran, which could protect them and favor environmental colonization [35, 36]. Furthermore, this capsular polysaccharide was proposed to entrap glucansucrase activity, explaining why the major part of the activity is recovered bound to the cell wall [37–39]. Six other strains of *L. citreum* sp. (LBAE A7, B7, C10, C12, K29, and K30), isolated from French sourdough, were also shown to produce dextrans with a high content of α-(1 → 2) linkages. As for *L. citreum* NRRL B-1299, glucansucrase activities were either soluble or associated with the cell wall [40–42].

Attempts to clone the enzyme involved in the α-(1 → 2) branched polymer formation started in the late nineties. Three glucansucrase encoding genes (*dsrA, dsrB, and dsrE*) were isolated [43–45]. Resulting recombinant DSR-A and DSR-B dextransucrases were shown to produce highly linear α-(1 → 6) linked dextrans. In contrast, DSR-E was much more atypical compared with other GH70 enzymes. With a molecular mass of 313 kDa, by far the highest molar mass described for a glucansucrase, DSR-E was further shown to be a bi-functional enzyme resulting from the assembly of two catalytic domains (CD1 and CD2) connected by a domain homologous to the glucan binding domain (GBD) of glucansucrases (rich in repeated motifs) [45]. Construction and biochemical characterization of DSR-E truncated forms proved that CD1 was responsible for polymerase activity, whereas CD2 was specialized in α-(1 → 2) transglucosylation from sucrose donor to dextran acceptor. Notably, the degree of α-(1 → 2) branching catalyzed by the bi-functional enzyme DSR-E never exceeded 5 %, a value much lower than that reported for the α-(1 → 2) branched polymer produced by the native strain [46, 47]. In contrast, the engineered forms derived from DSR-E, namely, GBD-CD2 and ΔN123 GBD-CD2 (a truncated version of GBD-CD2 that is deleted of 617 residues from the N-terminal extremity and results in a protein of 123 kDa), were really efficient for branching dextran up to 32 % in the presence of equivalent amounts of dextran and sucrose [48, 49]. Consequently, the high degree of branching naturally observed in NRRL B-1299 dextran was until recently attributed to the occurrence of degraded forms of DSR-E (comparable with GBD-CD2) in the fermentation broth of *L. citreum* NRRL B-1299 [46].

Another explanation can now be proposed, which results from the recent sequencing of *L. citreum* NRRL B-1299 genome [50]. This revealed the presence of three novel genes *dsrDP, dsrM, and brsA* coding for three GH70 enzymes named DSR-DP, DSR-M, and BRS-A [51]. Their biochemical characterization showed that DSR-DP and DSR-M are glucansucrases, whereas BRS-A catalyzes the α-(1 → 2) transglucosylation onto dextran as efficiently as the GBD-CD2 branching sucrase. The location of DSR-DP in a prophage provided the first evidence of a phage-mediated horizontal transfer in lactic acid bacteria. DSR-M and BRS-A were co-localized in the genome, in a region where tandems of GH70 enzymes are often found. DSR-M catalyzes short chain dextran synthesis. A high degree of α-(1 → 2) branching (up to 37 %) is obtained, suggesting that BRS-A is likely to be the main catalyst responsible for the in vivo branching of *L. citreum* NRRL B-1299 dextran. Thus, DSR-E would not be the major catalyst involved in α-(1 → 2) branched dextran synthesis. This hypothesis is reinforced by other genome sequence analyses. Indeed, *DsrE*-like genes (coding for two catalytic domains) were also identified in the genomes of *L. citreum* LBAE-C11, LBAE-E16, and LBAE-C10 (three strains isolated from sourdough). DsrE-like genes from LBAE-C11 and E16 share 99 and 97 % identity, respectively, with that of NRRL B-1299 [45, 52, 53], and code for two putative enzymes differing from DSR-E by only 11 and 35 deleted amino acids at the N-terminal end. However, neither strain converts sucrose into α-(1 → 2) branched dextran despite the presence of DSR-E-like enzymes (GSC11-2 and GSE16-2), raising the question whether these genes are functional or not. In contrast, *L. citreum* LBAE C10 is a strain known to produce a glucan rich in α-(1 → 2) glucosidic bonds, and its genome carries genes homologous to both *dsrE* and *brsA*. However, *Dsr*E-like gene is interrupted by three stop codons, probably resulting in a pseudogene [51], whereas the *brs*A-like gene is 99 % identical to *brsA*, and is predicted to encode a fully active protein. This latter seems to be the sole enzyme able to catalyze α-(1 → 2) linkage synthesis in this strain [41]. These findings argue in favor of a major involvement of the branching sucrase BRS-A in vivo. Analyses of the transcript level of the various genes found in *L. citreum* NRRL B-1299, as gene deletion combined with phenotypic characterization, are still required to provide more definite conclusions and understand the synergy occurring between

polymerases and branching enzymes during the course of highly α-(1 → 2) branched polymer synthesis.

Since 1950, another strain of *L. citreum*, *L. citreum* NRRL B-742, was known to produce a dextran polymer with a very high content of α-(1 → 3) branching (up to 50 %) [30, 54–56]. Looking for the enzymes possibly involved in the synthesis of this comb-like α-glucan, the genome of *L. citreum* NRRL B-742 was sequenced [50]. Genome annotation allowed identification of a new gene (*brs*B) encoding a putative GH70 enzyme sharing common traits with α-(1 → 2) branching sucrases. The recombinant forms of this enzyme (BRS-B) as well as a truncated version (BRS-BΔ1, with repeats at the C-terminal of the protein deleted) were efficiently produced in *E. coli*. Their characterization showed that they are specific for dextran branching via α-(1 → 3) linkage synthesis. Thus, starting from sucrose and a high molar mass dextran as acceptor (2×10^6 g mol^{-1}), the degree of α-(1 → 3) branch linkage went up to 50 %, indicating that this enzyme is likely to be involved in the highly α-(1 → 3) branched dextran synthesis. Indeed, the comb-like dextran synthesis is proposed to result from the action of at least one polymerase synthesizing a linear dextran (the genome contains three genes predicted to encode GH70 dextransucrases) and the α-(1 → 3) branching sucrase BRS-B. However, dextransucrases working in tandem with BSR-B have not been precisely identified yet [57].

Structural insight

Primary structure

Amylosucrases have been assigned to sub-family 13_4 of glycoside-hydrolases in which are also found sucrose-hydrolases [58]. Their sequences display the four conserved regions in which seven residues are highly conserved and play a critical role [59, 60] (Fig. 1). Among them are found the amino acids that constitute the subsite −1 of GH13 and that are involved in the α-retaining mechanism of action of these enzymes [61]. Using the *N. polysaccharea* amylosucrase numbering for illustration, these amino acids are: the nucleophile (D286), the acid–base catalyst (E328), the third aspartate (D393), and the two histidines (H187 and H392) involved the transition state stabilization. Two other highly conserved residues R284 and D182 correspond to important amino acids for structural integrity. Regions homologous to these signature sequences were also identified in the GH70 family, and parental relations between GH13 and GH70 enzymes were suggested as early as the nineties [62, 63] (Fig. 1). In particular, secondary structure prediction combined with sequence comparison allowed the prediction that GH70 glucansucrases adopt a $(\beta/\alpha)_8$ barrel structure revealing a circular permutation of the β1 to α3 secondary elements of the α-amylase barrel [64] (Fig. 2a). This was confirmed later with the resolution of the three-dimensional structures of GH70 enzymes [49, 65, 66].

In the conserved regions II, III, and IV where are found the three catalytic amino acids, the branching sucrases (GBD-CD2, BRS-A and BRS-B) share conserved residues, including F2214 (motif II, GBD-CD2 numbering), and I2317, H2319, K2323, and V2329 of motif IV. Other amino acids were uniquely found in BSR-B, including residues 673-IS of motif II, 711-PKGE of motif III, 796-IH of motif IV, and F1184 of motif I (Fig. 1, BRS-B numbering). Data mining based on the search for these motifs in GH70 enzymes allowed isolation of other putative branching sucrases, the enzymes BRS-C from *Leuconostoc fallax* KCTC 3537 and BRS-D from *Lactobacillus kunkei* EFB6. The recombinant production of these enzymes in *E. coli* and their biochemical characterization showed that both BRS-C and BRS-D act as branching sucrases with α-(1 → 3) and α-(1 → 2) transglucosylation specificity, respectively. These findings indicate that the conserved residues of motifs II and IV are good reporters of dextran branching ability in GH70 family, and that branching sucrases are not found only in *L. citreum* species [57].

Three-dimensional structures

GH13 amylosucrases

Several three-dimensional structures of *N. polysaccharea* amylosucrase (*Np*AS) in free form or in complex with various ligands (including sucrose, glucose, covalently bound glucosyl, maltoheptaose, and turanose complexes) [67–70] as well as two structures of *D. geothermalis* (*Dg*AS) and *D. radiodurans* (*Dr*AS) amylosucrases [71, 72] have been characterized. These enzymes are organized in five domains (Fig. 2). The domains A (residues 90–183, 260–394, and 460–553 according to *Np*AS numbering, which form the $(\beta/\alpha)_8$ barrel), B (*Np*AS residues 184–259 inserted between β-strand 3 and α-helix 3), and C (the all-β Greek key domain residues 554–628 in *Np*AS) are common to GH13 enzymes, whereas the N (residues 1–89 *Np*AS numbering) and B′ domains (*Np*AS residues 395–459 of an extended loop arising between β_7-strand and α_7-helix of the barrel) are specific to amylosucrases (Fig. 2b). In *Dr*AS and *Dg*AS, domains B and B′ are 4–5 residues longer than in *Np*AS. Notably, *Dr*AS and *Dg*AS crystals both revealed a dimeric assembly. This correlates with dimer formation in solution, which is suggested to enhance the stability of the two enzymes compared with *Np*AS and *Ac*AS (*Arthrobacter chlorophenolicus* amylosucrase), which exist

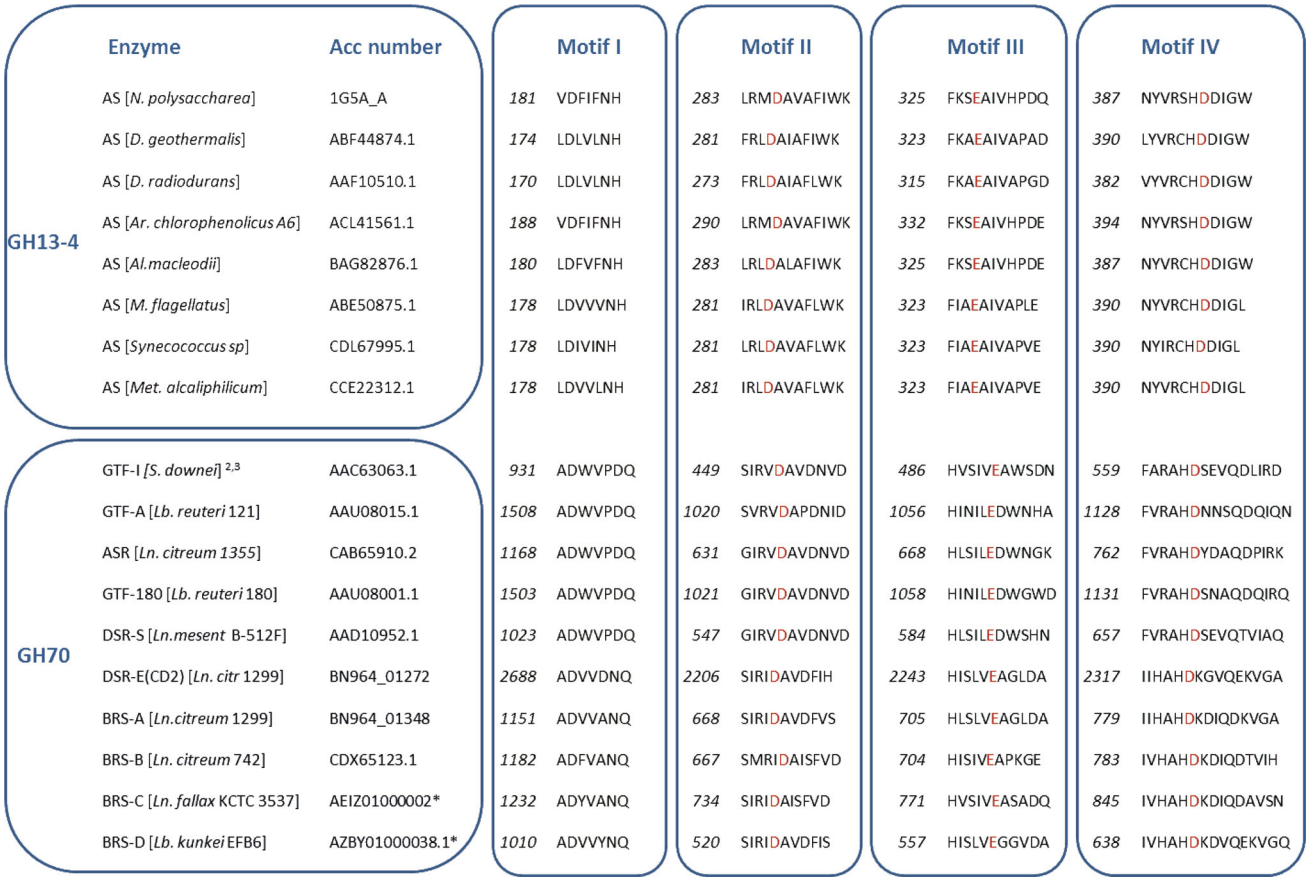

Fig. 1 Sequence alignment of the main conserved motifs in GH13 and GH70 families (motifs I to IV). Motif numbering refers to the motifs originally defined in the GH13 family. The two catalytic residues (in motifs II and III) and the transition-state stabilizer (in motif IV) are indicated in *red*. In GH70 enzymes, the sequence is permuted, so that motif I occurs after motif IV. Some sequences of GH70 polymerases are presented in addition to those of branching sucrases. For *Leuconostoc citreum* NRRL B1299, the accession numbers correspond to their locus tag on the genome (PRJEB5537). *Asterisks* for *Leuconostoc fallax* KCTC 3537, the enzyme is the resulting product of the ORF localized between positions 68,715–63,391 on the reverse strand. For *Lactobacillus kunkei* EFB6, the enzyme corresponds to the product of the ORF at locus tag: LAKU_38c00010

as monomers [20, 71, 72]. Mapping of the dimer interfaces of *Dr*AS and *Dg*AS further showed that a higher number of polar interactions and a better complementarity between the monomers are observed in *Dg*AS, which is also in agreement with the higher thermostability of *Dg*AS compared with *Dr*AS [17, 18]. Notably, *Dg*AS also contains a higher number of polar charged residues, a lower number of polar uncharged residues, and more hydrophobic and proline residues than *Np*AS, which were also proposed to contribute to the enhanced thermostability [18, 71]. Of the characterized amylosucrases, *Dg*AS remains the most thermostable with half-life times of 22 and 65 h at 50 and 30 °C, respectively.

*Np*AS superimposes on *Dg*AS and *Dr*AS structures with rmsd values of 0.9 and 1.5 Å for 462 Cα atoms and 472 Cα atoms aligned, respectively [71, 72]. More significant conformational changes are observed in *Dr*AS, the sole true free structure devoid of any ligand. *Dg*AS and *Np*AS active sites adopt a similar pocket topology at the bottom of which sucrose binds with the glucosyl and fructosyl rings occupying subsites −1 and +1, respectively [68]. A dense hydrogen bond network involving D286, H187, R284, D393, H392, as well as stacking interactions with Y147 and F250 (*Np*AS numbering) firmly maintains the glucosyl ring. Interactions with the fructosyl ring are scarcer, which accords with the necessity of fructose release during hydrolysis or transglucosylation. Fructosyl ring interactions involve hydrogen bonding with D393, D394, and R446 (*Np*AS numbering). It is noteworthy that the positions equivalent to D144, R509, D394, and R446 in *Np*AS are conserved in all amylosucrases and might be responsible for their substrate specificity. In both *Np*AS and *Dg*AS structures, the catalytic pocket is blocked at the bottom by a salt bridge formed between residues D144 and R509 (in *Np*AS numbering) conserved in all amylosucrases, which prevents the occurrence of −2, −3 subsites as logically expected for transglucosylases.

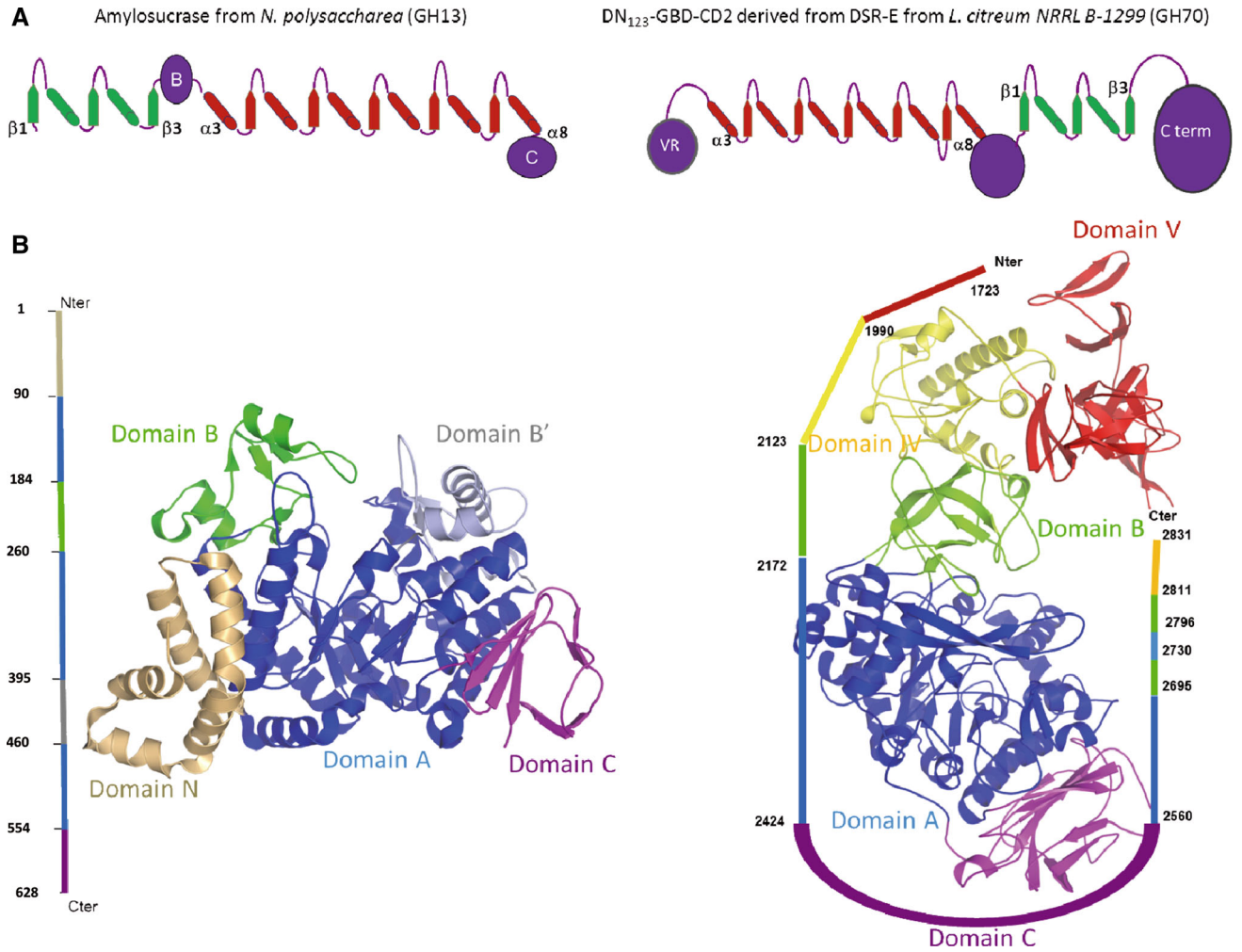

Fig. 2 Structural characteristics of *Np*AS and ΔN_{123}-GBD-CD2. **a** Topology diagrams of members of GH13 and GH70 families. *Cylinders* represents α-helices and β-sheets constituting the $(\beta/\alpha)_8$ barrel, and permuted elements are shown in green. **b** Schematic representation of the *Np*AS (PDB entry: 1G5A) and ΔN_{123}-GBD-CD2 (PDB entry: 3TTQ) structures with labeling and color-coding of the five domains (A, B, and C domains common to GH13 and GH70 enzymes; N and B′ for amylosucrases, domains IV and V for GH70 members)

The inactive mutant E328Q-*Np*AS/maltoheptaose complex (PDB entry: 1MVY and 1MWO) revealed three oligosaccharide binding sites OB1, OB2, and OB3 [69]. OB1 spans over the −1 and +1 subsites and includes five additional subsites (+2 to +6), ensuring a strong binding of the maltoheptaose residues. The OB2 and OB3 sites are positioned at the surface of B′ and C domains, respectively. As *Np*AS is very efficient for elongating glycogen branches [26], it was suggested that OB2 could assist amylose and glycogen anchoring during elongation. X-ray data of the complex between inactive mutant E328Q and maltoheptaose (G7) fragments bound at the OB1 and OB2 binding sites were used to model glycogen docking in *Np*AS active site and revealed that two residues of the B′ domain, F417 of OB2 and R415 of OB1 in subsite +4, could provide an anchoring platform to direct elongation of glycogen branches. Accordingly, mutation of these two residues decreased the enzyme activation usually observed in the presence of glycogen and restored maltooligosaccharide production from sucrose [73]. No function was attributed to OB3 so far. Of note, R226 of *Np*AS subsite +2 is replaced by a proline residue in *Dg*AS and *Dr*AS that liberates space [71]. Replacement of this residue by the 19 possible other amino acids, in *Np*AS, led to mutants, showing 1.5- to 6-fold increased activity compared with the wild-type *Np*AS. An autoactivation during catalysis was also revealed because of the improved binding of long maltooligosaccharides that enhance the de-glycosylation rate, resulting in much higher amounts of insoluble amylose formed [27, 74].

From soaking experiments of native *Np*AS with sucrose, a second sucrose binding site (SB2) with a moderate

affinity was revealed at the surface of *Np*AS just behind the salt-bridge. Most of the residues in contact with sucrose belong to the domain B′, suggesting that sucrose could enter the active site upon a large amplitude motion of this domain when glycogen branches occupy the OB1 site [68]. MD simulations of *Np*AS and *Dg*AS showed that loop 3 (B domain) and loop 7 (B′ domain) moved away from each other, thus opening the active site [71]. However, such large conformational rearrangements were never observed in the crystal structures of *Np*AS and *Dg*AS. The presence of a ligand in −1 subsite of all of the crystal structures is thought to force a closed conformation. In contrast and compared with *Np*AS and *Dg*AS structures, the crystal structure of *Dr*AS (the sole true free form) revealed a profound rearrangement around −1 subsite characterized by a disordered loop 2 that could not be modeled, as well as a shift of B and B′ domains that exposed −1 subsite to the solvent. Loop 2 disorder combined with B and B′ domain motions was attributed to protein flexibility rather than to proteolytic degradation. The consequence is that the salt bridge that closes up the active site was not formed in *Dr*AS structure. Opening of −1 and +1 subsites through such conformational changes could thus facilitate sucrose supply and fructose release while maintaining maltooligosaccharide acceptors or glycogen branches in proximity of +1 subsite, altogether these interpretations more generally raise the question of the dynamics of the transglucosylation reaction which is, up to now, far from being understood at the molecular level and necessitates further investigations.

GH70 GBD-CD2 branching sucrase

All attempts to crystallize the full length DSR-E failed. As a consequence, crystallization trials were rather focused on the second catalytic domain (CD2), specific for dextran branching, which was the most atypical with regard to linkage specificity. No crystals were obtained with the protein GBD-CD2 that contains the entire GBD and the second catalytic domain of DSR-E. Truncated forms with a reduced GBD were constructed. The shortest active one (ΔN123-GBD-CD2, 123 kDa; 1108 residues) was successfully crystallized. Two X-ray structures were solved at 1.90 and 3.3 Å resolution in different space groups [49]. In addition, three additional structures of native ΔN123-GBD-CD2 in complex with glucose, isomaltose, and isomaltotriose were recently released (PDB entries: 4TVD, 4TTU, 4TVC).

The 3D-structure of the α-1,2 branching sucrase ΔN123-GBD-CD2 is organized in five domains (A, B, C, IV, and V) like the 3D-structures of glucansucrases GTF180-ΔN from *Lactobacillus reuteri* 180 [65] and GTFA-ΔN from *Lactobacillus reuteri* 121, which were, respectively, deleted of 741 and 739 amino acids at their N-terminal extremity (ΔN) for crystallization [75] (Fig. 2b). The enzyme adopts the typical U-shape fold encountered in this family. The A, B, IV domains result from the three dimensional organization of non-contiguous fragments of sequence, whereas the domain C consists of one continuous polypeptide segment (G2425 to D2560) at the bottom of the U-fold. The domain A is built up of three polypeptide segments (L2173-S2424, S2561-V2695, and G2731-S2796). As in GTF180-ΔN and GFT-SI, these fragments form the $(\beta/\alpha)_8$ barrel in which the catalytic cleft is situated and reveal a circular permutation compared with GH13 family barrel [65, 66] (Fig. 2a). The domain A also displays some specific traits, and helix α5 is shorter than in GTF180-ΔN and GTF-SI. The loops from G2731 to S2796 and from D2292 to I2299 are 25 and 4 residues longer, respectively, than their homologues in GTF180-ΔN. These loops are specific to GBD-CD2 but their involvement in the enzyme specificity has not been investigated yet. Domain B results from the assembly of three polypeptide segments (R2124-L2172, Y2696-V2730, and W2797-G2811), and is comprised of a five-stranded β-sheet that superimposes well on the domain B of GTF180-ΔN, with 94 Cα aligned out of 99 Cα. However, one loop inserted between R2157 and F2163, at the upper part of the catalytic cleft, is eleven residues shorter than its counterpart in GTF180-ΔN. Domain IV consists of two polypeptide segments (D1991-N2123; M2812-T2831) and appears to be specific to the GH70 family from DALI analysis. Finally, domain V of ΔN123-GBD-CD2 is formed by only one single continuous fragment (A1723-L1990) emerging at the N-terminal of the protein [49], contrary to domains V of GTF180-ΔN and GTF-A-ΔN that are composed of fragments from the N and C-terminal extremities.

Superimposition of ΔN123-GBD-CD2 with GTF180-ΔN:sucrose complex revealed a good conservation of the residues defining the subsites −1 and +1 with 17 residues aligning with an rmsd of 0.53 Å on Cα. Moreover, a glucose molecule was found in the presumed −1 subsite in the recently released ΔN123-GBD-CD2:glucose complex (PDB entry: 4TVD). The molecule interacts with residues R2208, D2210, E2248, H2321, D2322, D2643, and Y2650, which are all conserved in GH13 family. By analogy, residues D2210, E2248, and D2322 were putatively assigned the role of nucleophile, acid–base catalyst and transition state stabilizer, respectively. Two other residues, Q2694 and D2643, are also hydrogen bonded with the O4 and O6 of the glucosyl ring, as observed in GTF180-ΔN:sucrose complex. Q2694 is equivalent to *Np*AS residue H187 that assists catalysis by stabilizing the transition state [70, 76]. In −1 subsite, residues D2643 and N2596 (corresponding to D1458 and N1411 residues in GTF180) could also be responsible for the closure of the subsites −2 and −3, but this should be verified by mutagenesis.

No sucrose complexes were obtained with ΔN123-GBD-CD2. However, the residues L2166, L2167, E2248, D2322, and Q2326 adopt the same position as in GTF180-ΔN subsite +1 suggesting that, as observed for GTF180-ΔN, the two leucine residues of the B domain could interact through van der Waals interactions with the fructosyl moiety, and that Q2326 could be H-bonded with the O6 of the fructosyl ring [49]. In GTF180-ΔN:sucrose complex, the fructosyl ring of sucrose also establishes weak interactions with N1029 and W1065 [65]. These two residues are strictly conserved among the characterized GH70 glucansucrases. In ΔN123-GBD-CD2, N1029 is substituted by F2214 (also conserved in BRS-A and BRS-B) and W1065 superimposes with neither A2249 nor G2250, although it aligned correctly with G2250 in sequence alignments. Consequently, these residues are not correctly positioned to interact with the fructosyl ring that would be rather maintained via H-bond between K2323 (equivalent to K 789 in BRS-B) and O4. Overall, this suggests a weaker binding of sucrose in branching sucrases compared with glucansucrases. The residues F2214, A2249, and G2250 were mutated to restore the motifs of glucansucrases. Four mutants were constructed A2249W, G2250W, A2249D/G2250W, and F2214N [49]. All of them still consumed sucrose but with significantly reduced hydrolytic activity. However, no polymerization activities were detected, indicating that more complex modifications are necessary to change a branching sucrase into a glucansucrase, and vice versa. Notably, residue F2214 appeared critical for dextran binding and branching, as mutant F2214 N was unable to use 1 kDa dextran as an acceptor, in contrast with the wild-type enzyme.

The ΔN123-GBD-CD2:glucose complex revealed in total 9 glucose binding sites (PDB entry: 4TVD). Four of them are located in the domain A (including −1 subsite) and the others in the domains B, IV, and V. The functional significance of these sites remains to be established, considering that their abundance on the protein surface is probably not fortuitous for a dextran-branching enzyme showing protein/dextran Kd estimated, by affinity gel electrophoresis, at 0.3 and 104 μM for dextrans of 22.5 MDa and 68.4 kDa, respectively. Two other structures in complex with isomaltosyl and isomaltotriosyl units were also recently solved, at 2.2 and 1.85 Å, respectively, from soaking experiments with isomaltotriose or glucooligosaccharides (PDB entries: 4TTU and 4TVC). Electron density corresponding to glucose, isomaltosyl and isomaltotriosyl groups, was uniquely observed in domain V, providing the first evidences of molecular interactions occurring between carbohydrates and the domain V of GH70 enzymes. Domains V are non-catalytic domains found in almost all GH70 enzymes at the N and/or C-terminal extremities of domain IV [1]. In GBD-CD2, domain V is composed of one fragment of sequence situated at the N-terminal, whereas in BRS-A and BRS-B, sequence analyses suggest that domain V could be formed by two discontinuous fragments at N- and C-terminal ends. The ability of GH70 domain V to bind dextran was first shown with non-catalytic tryptic digests of several streptococcal glucansucrases [77]. Sequence analyses suggested that dextran binding was related to the presence of repeated motifs, which were classified in different groups [78–82] and proposed to have evolved from a common YG repeat [83]. Several studies report that some domains V separated from their catalytic domains also bind dextran [84–87], which demonstrates that domains V can fold in an autonomous way. Very low Kd in the range of nM were described. However, these reported Kd values cannot be easily compared due to variations in the sequences and numbers of the repeated motifs. ΔN123-GBD-CD2 branching sucrase was recently proved to bind dextran and the presence of isomaltosyl and isomaltotriosyl groups in the domain V of the crystal structures 4TTU and 4TVC suggest that domain V is involved in dextran binding. However, it is difficult to distinguish the binding contribution of the catalytic domain and that of the domain V to Kd values. Truncated forms devoid of the catalytic domain should be constructed and tested for their binding ability to estimate the Kd value of dextran due to interactions with domain V only.

Domain V of GBD-CD2 adopts a modular β-solenoid fold that superimposes well with domain V of the crystal form GTF-180ΔN-II [49, 88]. The protein is compact. Domain V is in interaction with domains B and IV and is rotated by 120° relative to the location of domain V in GTF-180ΔN-I that crystallized in a different space group and is more extended [65]. The two crystal forms of GTF-180ΔN as well as SAXS experiments provided the first evidence of conformational flexibility of domain V around a hinge located between domain IV and V, which is conserved in ΔN123-GBD-CD2, indicating that a similar flexibility could exist in the branching sucrases [88]. The analysis of the complexes of ΔN123-GBD-CD2 obtained with glucose, isomaltose, and isomaltotriose allowed the study in more detail of the topology of two sugar pockets named V-K and V-L. These pockets comprised approximately 80 residues and are defined by three supersecondary motifs of either β-hairpins or three-stranded antiparallel β-sheets and were exposed to the solvent. Typically, the three glycosyl rings (Glc1, Glc2, and Glc3) of isomaltotriose group found in V-K pocket were maintained through stacking interaction between Glc2 and Y1834 and hydrogen bonds with W1849, Q1870, Q1879, K1881, G1897, and K1898 (Fig. 3). Residues Y1834, K1881, Q1879, and K1898 were conserved in the V-L pocket that bound glucose, suggesting that these pockets

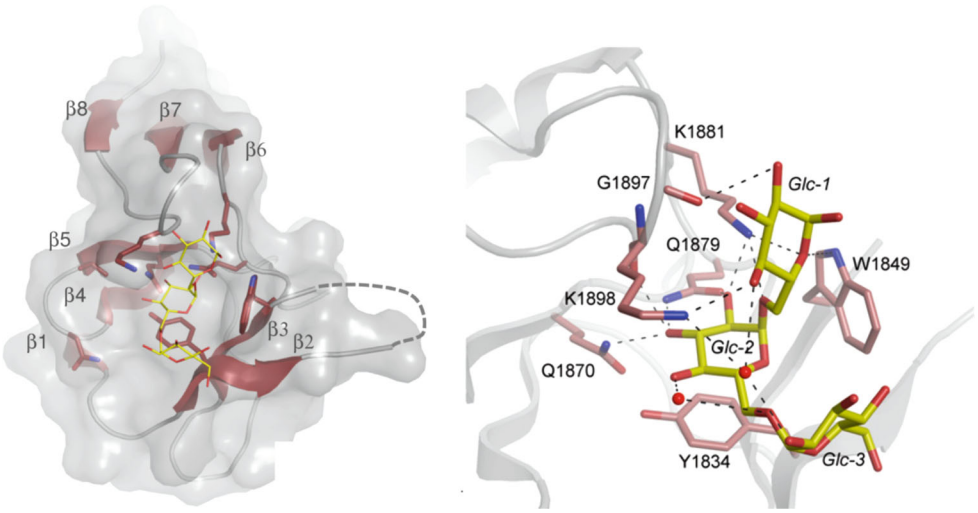

Fig. 3 Representation of the sugar binding pocket K in domain V of ΔN_{123}-GBD-CD2 (PDB entry 4TVC). *Left* molecular surfaces are shown in *light gray*, and bound isomaltotriose is represented in *yellow lines*. *Right* zoom on the amino acids involved in interactions with isomaltotriose

may contribute together to binding of longer dextran chains, but structural evidences are still lacking. Sequence and structural alignments further allowed identification of similar pockets in GTFA-ΔN and GTF-180ΔN, as well as in domains V of other GH70 enzymes that were proved to independently bind dextran [84–87]. Sequence analysis was extended to the entire domain of DSR-E allowing the identification of ten putative binding pockets. The role of these binding pockets in dextran elongation or branching remains to be investigated. In GBD-CD2, the entire deletion of domain V totally abolished branching activity, whereas maintaining a part of domain V in ΔN123-GBD-CD2 results in an enzyme as efficient as GBD-CD2, indicating that domain V and its sugar binding pocket are important for branching activity and may act in synergy with the catalytic domain [46].

Mechanism, product profile, and kinetics of GH13 amylosucrases and GH70 branching enzymes

Reactions with sucrose alone

Amylosucrases follow the double-displacement mechanism common to all enzymes of the GH13 family (Fig. 4). In the first step, the donor binds at the bottom of the catalytic pocket with the glucosyl ring occupying the −1 subsite and the fructosyl ring the +1 subsite. Next, the acid/base (E328 in *Np*AS) assists the nucleophilic attack exerted by the aspartate nucleophile (D286 in *Np*AS). The reaction goes through the formation of an oxocarbonium ion leading to formation of the covalent β-glucosyl-enzyme intermediate and fructose release. In the second step, the deprotonated acid–base catalyst serves as base to activate the hydroxyl group of an acceptor molecule, which can be either water (hydrolysis reaction) or an acceptor (transglucosylation). Km values for sucrose are in the range of mM. Ratio of transglucosylation versus hydrolysis initial rate varies among amylosucrases from 0.26 for *Sy*AS (amylosucrase from *Synechococcus* sp.) [23] to 1.8 for *Am*AS (amylosucrase from *Alteromonas macleodii)* [21], the amylosucrase from *Synochococcus* being the less efficient transglucosylase. The values reported for amylosucrase specific activity range from 400 (*Am*AS) to 0.005 U/mg (*Sy*AS) depending on the enzyme source and temperature. The molecular traits at the origin of these variations remain to be investigated.

Amylose-like formation was shown to result from successive transglucosylations occurring at the non-reducing end of maltooligosaccharides through a multi-chain process of elongation [27]. Glucose is first released from sucrose hydrolysis and then acts as acceptor to yield maltose which in turn will be glucosylated and so forth. Sucrose isomers, turanose and trehalulose, are also usually synthesized. They result from transfer of the glucosyl units to fructose. The relative amount of isomers is dependent on the enzyme. *Np*AS synthesizes preferentially turanose, whereas *Dg*AS produces equal amounts of trehalulose and turanose. *Dg*AS and *Np*AS turanose complex analysis revealed that two residues (R226 and I330 in *Np*AS numbering) are likely responsible for the preferential formation of turanose by *Np*AS. In *Dg*AS, R226 is not conserved, and the equivalent of I330 is not similarly placed. These topologic changes give thus more flexibility for fructose accommodation that could account for the amount of trehalulose produced by *Dg*AS [71]. Notably, the formation of sucrose isomers can be significantly increased up to 50 % by using high sucrose concentration [89] or by adding fructose acceptor in the reaction mixture [71]. The profile of products obtained from *Np*AS and *Dg*AS has been fully

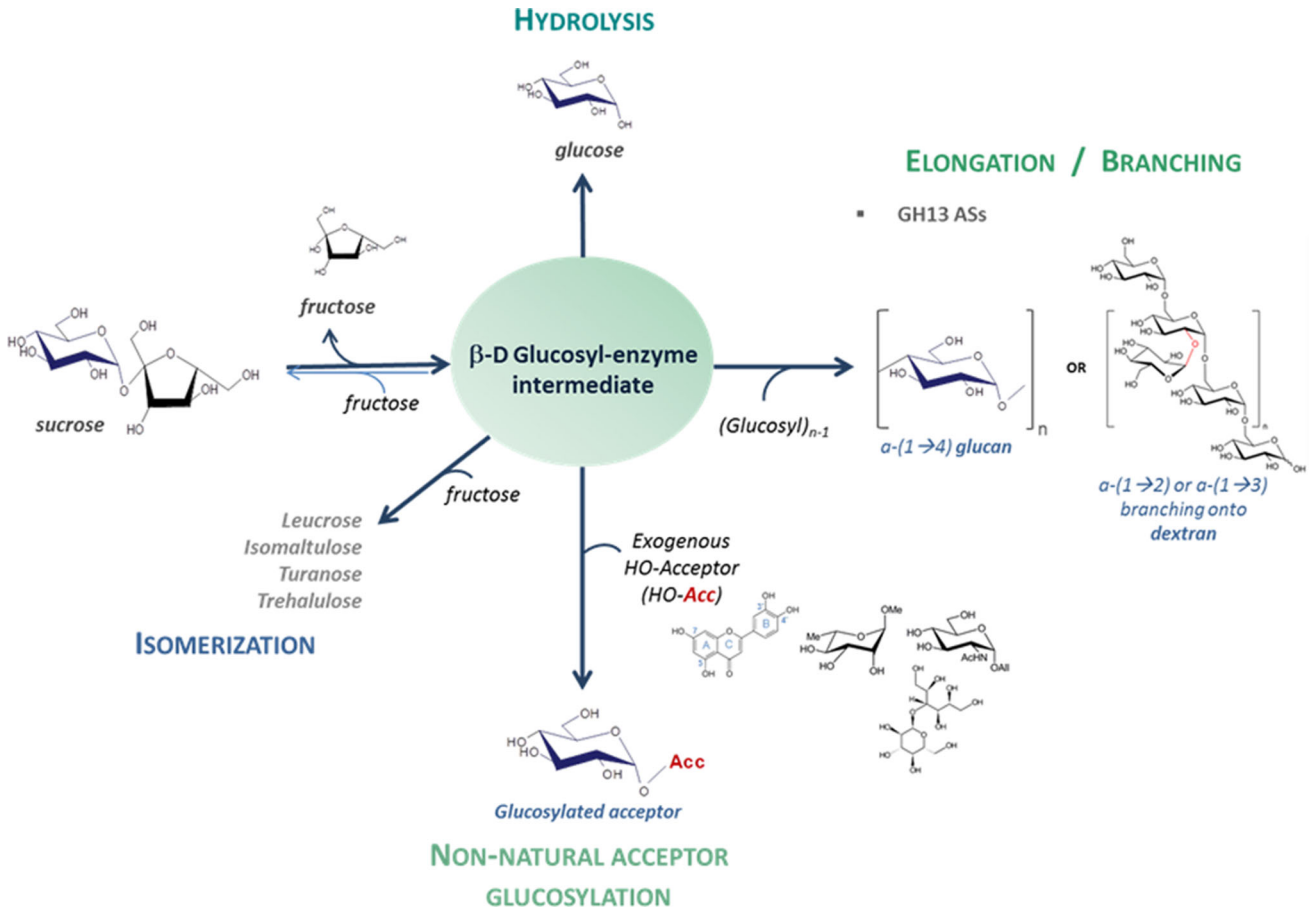

Fig. 4 Main reactions catalyzed by α-transglucosylases from GH13 and GH70 families. Structures of luteolin, L-rhamnose, *N*-acetyl-glucosamine, and maltitol are shown as an example of exogenous acceptors

described. Typically, in *Np*AS, the glucosyl residues issued from 100 mM sucrose are retrieved in glucose (4 %), sucrose isomers (19 %), soluble (20 %), and insoluble maltooligosaccharides (57 %). Degree of polymerization of the α-(1 → 4) linked-chains can go up to 80 and precipitation occurred during the course of the reaction due to chain self-association. Yield, morphology, and degree of crystallinity of insoluble amylose can be modulated by varying sucrose concentration. All types of particles exhibit an exceptionally high B-type crystallinity conjugated to a high resistance to digestive enzymes and valuable fiber properties [90]. The conformational changes of amylose during reactions catalyzed by *Np*AS and *Dg*AS were tracked by SAXS experiments. At the early stage, amylose produced by *Np*AS and *Dg*AS associates in worm-like double helical cylindrical structures that later form clusters and aggregates that precipitate. With *Dg*AS, amylose chains did not entangle to yield aggregates in the experimental conditions used. The reaction was monitored at higher temperature than with *Np*AS, preventing self-association in clusters [91].

With the view of designing α-glucans with controlled properties, *Np*AS was also used in tandem with the branching enzyme from *Rhodothermus obamensis* to establish a biomimetic system of glycogen synthesis from sucrose only. By adjusting sucrose concentration and the ratio of branching enzyme versus elongating enzyme, hyperbranched polymers varying in size (10–150 nm), branching degree (10–13 %), and molar mass (3.7×10^6–4.4×10^7 g mol^{-1}), and showing similarity to glycogen were obtained. Their detailed characterization (involving enzymatic cleavage of external branches, chromatographic analysis, transmission microscopy, and asymmetrical flow field flow fractionation (AF4) coupled to quasi-elastic light scattering) showed that these polymers have a more homogeneous branching pattern than that of glycogen [92, 93]. Of note, amylopectin-like polymers could not be synthesized with this approach. Another original combination of enzymes involving amylosucrase was recently proposed for the production of trehalose, an important disaccharide in the food industry [94]. The process was based on the use of *Dg*AS simultaneously or successively

with a fusion protein (MTSH) made up of the maltooligosyltrehalose synthase (MTS) and the maltooligosyltrehalohydrolase (MTH) from *Brevibacterium hevolum*. MTS was expected to convert the α-(1 → 4) linkage of the maltooligosaccharides produced by *Dg*AS into an α-(1 → 1) linkage, and to produce maltooligosyltrehalose that was known to be cleavable to give trehalose and maltoligosaccharides with MTH. From 20 mM sucrose and without any optimization, the trehalose production yield attained 14 % in one pot reaction, and 31.5 % when *Dg*AS and MTSH were used in cascades.

The residues lining OB1 binding site are important for maltooligosaccharide elongation. In *Np*AS, mutation of D394 and R446 into alanine resulted in enzymes that were less active on sucrose (23.5 and 15 %, respectively, compared with the wild-type enzyme) and lost their ability to produce long chain maltooligosaccharides [27]. High-rate segmental random mutagenesis was also applied to the sequence fragment from R390 to G396 of *Np*AS containing residues of subsites −1 to +3. Of a library of 1000 variants, only 6.8 % of the clones retained sucrose cleavage ability. Most of these clones (82 %) were unable to produce iodine-stainable products. Analyses of the mutant deficiency for polymer elongation revealed that mutations at position 394 and 396 were critical to maintain elongation of maltose and/or maltotriose [95]. In a similar way, R415A mutation terminated elongation at the maltotetraose stage, confirming the role of R415 that provides a stacking platform at subsite +4 shown to be crucial for chain elongation [27]. All these mutants are promising candidates to generate transglucosylation products devoid of long chain amylose. In contrast, introduction of mutations at position 226 of *Np*AS allowed improved amylose formation up to 80 % by reducing steric hindrance and facilitating deglucosylation steps by maltooligosaccharide acceptors [27, 74].

When using only sucrose as substrate, the GH70 branching sucrases do act almost exclusively as hydrolases with specific activities around 35 U/mg. Approximately 10 % of the glucosyl residues of sucrose are also transferred to fructose to yield leucrose. Additional small size oligosaccharides were also identified by HPAEC analysis. Their structures have not been elucidated to date due to their very low amount of production [51, 57].

Reactions with sucrose and amylaceous or dextran polymers

Steady-state kinetics of *Np*AS in the presence of glycogen, proposed to be the natural acceptor of amylosucrase, showed that the reaction rate progressively increases with increasing glycogen amounts. A 100-fold increase in the initial velocity was observed with 30 g/L glycogen and 34.2 g/L sucrose as compared with the value obtained with sucrose only. In these conditions, linear amylose synthesis is considerably reduced down to 1 %, to the profit of extension of glycogen branches [26, 96]. Accordingly, morphology of the modified glycogen was shown to be highly dependent on the sucrose/glycogen weight ratio. At high ratio (34.2/0.1 g/L), dendritic nanoparticles are obtained, which show a 4–5 increased diameter compared with the initial particle. Linear amylose is also co-synthesized and all the products revealed a B-type crystal structure [96]. At low ratio (34.2/30 g/L), glycogen branches were less elongated yielding a polymer similar to glycogen, but less homogeneous, and showing small crystallites at the surface of the glycogen particles. *Np*AS was also shown to modify other amylaceous products, such as amylopectin, waxy-maize starch (phytoglycogen), limit dextrins, hydrothermally treated flours, rice starch, and barley starch [97–99]. After *Np*AS action, the resistant starch content increases, emphasizing the potential of amylosucrase treatment to modulate the digestibility of a wide range of amylaceous products.

Dextran is the natural acceptor of the branching sucrases. A steady-state kinetic analysis conducted with sucrose and 70-kDa dextran showed that the enzyme GBD-CD2 displays a ping-pong bi–bi mechanism of transglucosylation, for sucrose concentrations ranging from 10 to 300 mM. Notably, transglucosylation velocity is much higher than that for hydrolysis [48]. The k_{cat} value of transglucosylation reaction was estimated at 970 s^{-1}, one of the highest catalytic constants ever reported for glucansucrases, suggesting that dextran may accelerate deglucosylation of the glucosyl–enzyme intermediate. Of note, the kinetic parameters of the truncated forms ΔN123-GBD-CD2 and BRS-B-Δ1 were close to those determined for GBD-CD2 [48, 51]. Furthermore, the degree of α-(1 → 2) or α-(1 → 3) linkages incorporated in dextrans was shown to be controllable by the initial [sucrose]/[dextran] molar ratio [48, 51, 57]. Thus, by varying this ratio from 0.92 to 4.74, the degree of α-(1 → 2) branching varies from 10 to 30 %, respectively. With BRS-B, the branching degree can reach 50 %, every glucosyl unit of the chain being branched by one additional glucosyl unit. Investigation of the kinetics of oligosaccharide branching further revealed that the branching process of GBD-CD2 is stochastic and that linear oligosaccharides can bind at the active site in various ways, as revealed by the profile of branched oligosaccharides formed during the reaction course [100]. The α-(1 → 2) branched oligosaccharides with 10 of 30 % of α-(1 → 2) linkages are highly resistant to digestive enzymes [101]. Furthermore, they were shown to be metabolized by various species of beneficial gut microbiota [5, 102, 103] and to promote change in gut microbiota of mice and metabolic adaptation independently

of their genetic background and diets [104, 105]. All these properties indicate that α-(1 → 2) branched products may be promising dietary fibers.

Glycodiversification with GH13 AS

Glucoconjugates and oligosaccharides play an important role in host-defense, cell–cell recognition, ligand–receptor binding, and cell signaling. They find numerous applications as therapeutics, food ingredients, and/or fine chemicals. However, their chemical synthesis can be tedious due to the lack of regiospecificity of glycosylation reactions, thus requiring multiple protection–deprotection steps of reactive hydroxyl groups under harsh conditions that limit yields and production rates. In this context, enzymatic synthesis offers an attractive alternative, thanks to the regioselectivity and stereoselectivity of enzymes and their mild reaction conditions. While most of the effort has been concentrated on dextran branching, the glycodiversification and glucosylation of unnatural acceptors with branching sucrases have not been investigated yet. In contrast, the ability of amylosucrases to glucosylate exogenous acceptors has been widely explored to produce novel carbohydrate-based molecules [2].

Glycosylation of sugars and polyols

To get better insight into the donor and acceptor ambiguity of *Np*AS, twenty non-native acceptors, including L- and D-monosaccharides (arabinose, galactose, altrose, fucose, xylose, allose, and mannose) and sugar alcohols (D-sorbitol, xylitol, D-arabitol, D-mannitol, myo-inositol, and maltitol), were tested for glucosylation [16, 106]. Of the 20 acceptors, 19 were glucosylated to various degrees ranging from 3 to 100 % with the exception of L-fucose, thus highlighting the remarkable plasticity of *Np*AS subsite +1. Interestingly, the comparison of glycosylation levels of L- and D-monosaccharides clearly underlines the enantiopreference of *Np*AS, which could also be exploited for racemic resolution of diverse types of hydroxylated molecules. Depending on the acceptor, single or polyglucosylation was observed as well as new linkage specificity. This was attributed to the compatibility between the topology of subsite +1 and the acceptor conformation, which is the determinant to force the acceptor molecule to adopt the most suitable conformation for productive catalysis. A deoxysugar, 2-deoxyglucose, was efficiently elongated with *Np*AS to generate traceable material used to analyze glucose absorption from starch digestion in human gut. Results indicate that interactions with O_2 are not critical for a correct positioning in subsite +1 [107]. Trans-piceid glucosides (a glucosylated form of resveratrol) were also synthesized with *Am*AS or *E.coli* cells producing *Am*AS with 35 % and 75 % conversion yields, respectively [108]. Glucosyl transfer occurred on the glucosyl unit of trans-piceid through the formation of an α-(1 → 4) linkage and enhanced trans-piceid solubility. Glycerol was also shown to be glycosylated by *Methylobacillus flagellatus* amylosucrase (*Mf*AS) yielding three products: (2S)-1-*O*-α-D-glucosyl-glycerol or (2R)-1-*O*-α-D-glucosyl-glycerol and 2-*O*-α-D-glucosyl-glycerol [22].

Glucosylation of flavonoids

Flavonoids represent an important class of plant secondary metabolites. Thousands of structures have been identified, which provide protection against UV radiation, pathogen infections, or are involved in plant colors [109]. Furthermore, a continuously increasing number of studies show that flavonoid-rich diets are associated with a low incidence of chronic diseases, such as cardiovascular diseases, type II diabetes, neurodegenerative diseases, and possibly cancers. Thus, interest in understanding the relation between flavonoid structure, reactivity, and health benefits has rapidly increased over the past decades [110]. Notably, the presence of one or several sugars attached to the flavonoid backbones significantly impacts their properties, in particular their solubility, stability, bioavailability, and their biological activities [111, 112]. These findings have greatly stimulated the search for new flavonoid glycosides and the exploration of novel enzymatic routes of synthesis to facilitate their production and investigate their properties as new medicines, functional foods, or cosmetics. An active field of research deals with in vitro glycosylation using natural or engineered uridine diphosphate-dependent glycosyltranferases (UGTs), the natural catalysts involved in flavonoid glycosylation [113].

As nucleotide sugars are expensive substrates, the use of glycoside-hydrolases represents an interesting alternative pathway to flavonoid glycosides that is actively explored, especially with glucansucrases from GH13 and GH70 families [2, 114]. Using these enzymes for glucodiversification of flavonoids is also advantageous due to the fact that they give access to α-derivatives that are very rarely found in plant material. The potential of glucansucrase usage for flavonoid glucosylation was first demonstrated by Nakahara et al. [115]. They converted 0.55 mM (160 mg/L) of (+)catechin into catechin glucosides from 4-mM catechin and 60-mM sucrose. Later, Meulenbeld et al. compared the efficiency of catechin glucoside formation using several recombinant glucansucrases from *Streptococcus sobrinus* SL-1 and *Streptococcus mutans* GS-5—(GTF-B and GTF-D) [116]. GTF-D exhibited the highest efficiency, with a (+)-catechin conversion rate of approximately 80 % yielding 7.9 mM of (+)-catechin glucosides

from 10-mM catechin and 100- or 60-mM sucrose. Three flavonoid glucosides were obtained [(+)-catechin-4′-*O*-α-D-glucopyranoside, (+)-catechin-4′,7-*O*-α-di-D-glucopyranoside, and catechin-7-*O*-α-D-glucopyranoside] indicating that glucosylation could target ring A or B of flavonoids [116, 117]. Successful glucosylation of luteolin [118], myricetin [118], quercetin [118, 119], epigallocatechin [119, 120], ampelopsin [120], and astragalin (kaempferol-3-*O*-β-D-glucopyranoside) [121] with dextransucrases from *L. mesenteroides* sp was later reported. When investigated, the solubility of the flavonoid glycosides was always improved compared with that of aglycons.

The use of amylosucrases for flavonoid glucosylation was first reported in 2011 by Cho et al. [122]. *Dg*AS was employed to convert 90 % of (+)-catechin into catechin glucosides from 25-mM (+)-catechin and 25-mM sucrose donor. Two major products were obtained, i.e., (+)-catechin-3′-*O*-α-D-glucopyranoside and (+)-catechin-3′-*O*-α-D-maltoside. The presence of maltooligosyl (+)-catechin was also identified. The enzyme was also shown to catalyze the glycosylation of hydroquinones yielding a-arbutin with 90 % conversion using 10:1 sucrose/hydroquinone ratio [123, 124]. Baicalein-6-α-glucoside was also produced with *Dg*AS from sucrose and baicalein (a flavonoid extracted from the roots of *Scutellaria baicalensis* and used against infections and inflammatory diseases in Asia) [125]. This compound was 26 times more soluble than the aglycon and was more resistant to chemical and enzymatic oxidation, suggesting that it could be a good substitute of baicalein as a therapeutic drug. Glucosylation by *Np*AS of phloretin, a dihydrocalchone occurring in plants, was also recently reported. Phloretin α-glucosides were more soluble and showed a reduced cytotoxicity compared with the aglycon [126].

Flavonoid glucosylation with amylosucrases and GH70 enzymes highlights the remarkable plasticity of glucansucrase acceptor subsites. No doubt that, in the future, such glucosylation processes will be applied to larger sets of polyphenolic compounds. However, although broad, the acceptor promiscuity of these enzymes is nevertheless limited. Enzymes have not naturally evolved to transform non-natural acceptors and may not even exist in nature. To overcome these current limitations, progress in genomics, bioinformatics, protein computational design, enzyme engineering, and high-throughput screening of carbohydrate-active enzymes offers profitable and versatile solutions [127]. First, the immense and continuously growing reservoir of gene and protein databanks can be consulted, and high-throughput functional genomics and metagenomics can be performed to decipher promiscuity and hopefully find an enzyme with the required property. Another alternative is to take advantage of protein engineering, supported by impressive advances in in vitro enzyme evolution and computationally guided design [128, 129]. In particular, computer-aided approaches, including sequence alignments combined with or without structural data, phylogenetic analyses, and identification of mutation correlations within protein superfamilies, occupy a prominent place in the rationalization of enzyme evolution to design focused libraries, guide amino acid substitutions, and narrow down the size of the library [130]. In addition, a computational protein design allowing total in silico conception of new-to-nature enzymes is developing quickly with outstanding achievements [131, 132].

Engineering specificity toward non-native acceptors

In the last decade, engineering of amylosucrases has mainly targeted the development of chemo-enzymatic routes for the synthesis of complex carbohydrates. Such synthesis is often hampered by the lack of appropriate enzymatic tools having the required substrate specificity for new reactions, especially those envisaged to enter at a programmed stage of a chemo-enzymatic synthesis. This concept was investigated to explore the development of chemo-enzymatic pathways dedicated to the synthesis of O-antigenic oligosaccharides mimicking the lipopolysaccharide of Gram negative *Shigella flexneri* pathogenic strains. Such fragments could enter into the development of carbohydrate-based multivalent glycovaccines against Shigellosis, also called bacillary dysentery, which is among the four major causes of diarrheal disease in children under 5 years old and for which no vaccines and, *a fortiori,* no multivalent vaccines are yet available [133].

The *S. flexneri* O-antigen is formed by a pentasaccharide repeating motif encompassing a tetrasaccharide backbone composed of three L-rhamnopyranosyl units (A,B,C) linked by α-(1 → 2) and α-(1 → 3) glucosidic linkages and attached to *N*-acetyl-glucosamine (D) by an α-1,3 linkage (Fig. 5). This linear tetrasaccharide is usually decorated with either a glucosyl unit or an O-acetyl group [134], the position and regiospecificity of the glucosylation being specific to each serotype. At an early stage of development, the introduction of the α-D-glucopyranosyl side-chains featuring in all relevant *S. flexneri* polysaccharides was seen as the most limiting factor for the development of efficient syntheses of type-specific O-Ag fragments. Instead of relying on the strongly membrane-associated *S. flexneri* type-specific glucosyl transferases [135] to achieve the required high stereoselective and regioselective α-D-glucosyl introduction, the potency of *Np*AS amylosucrase was first examined. A structurally guided approach was conducted to engineer the required biocatalysts from *Np*AS. According to molecular modeling studies and

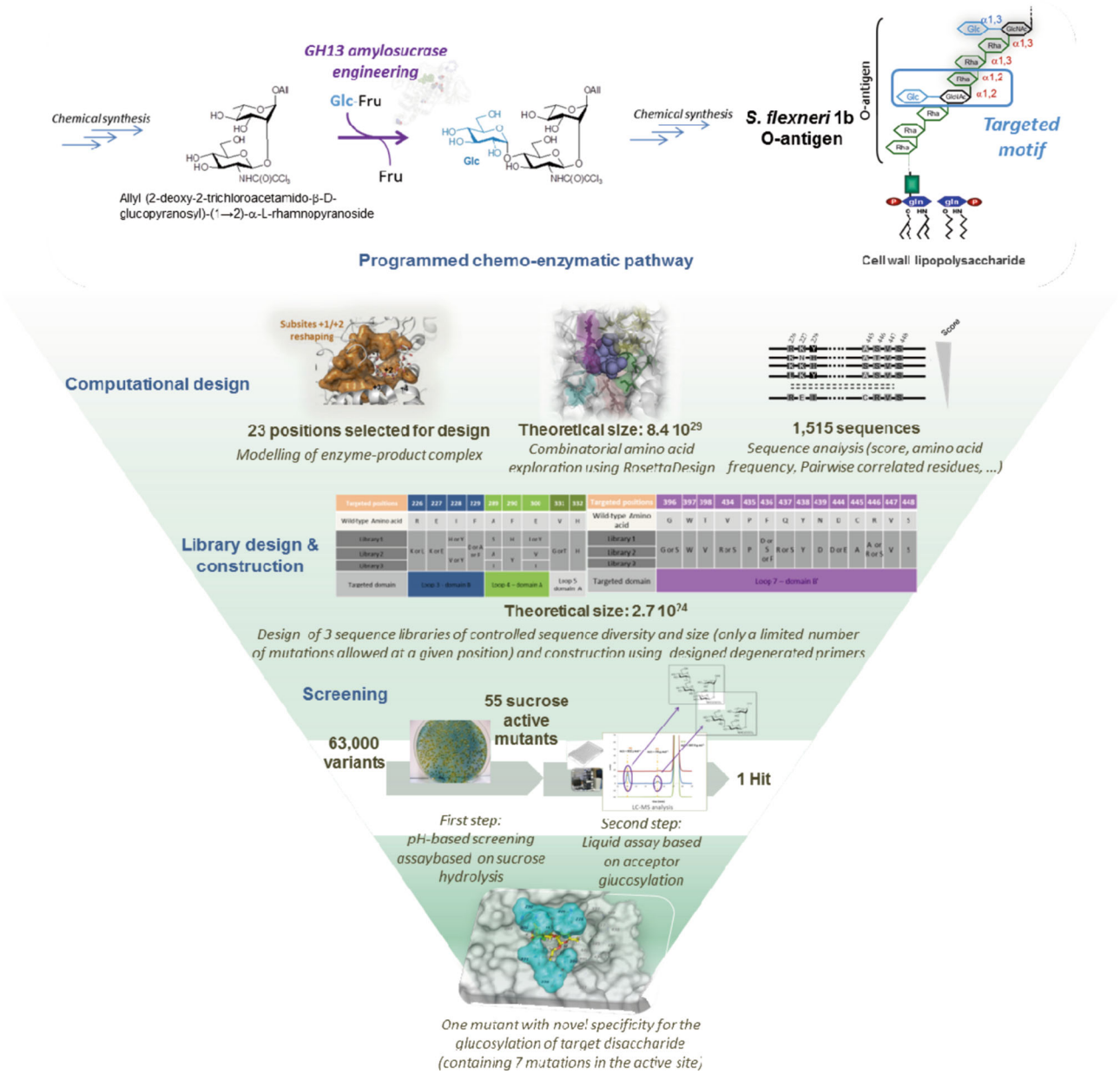

Fig. 5 Computer-aided strategy applied to engineer *Np*AS amylosucrase for the glucosylation of a disaccharide of relevance for the chemo-enzymatic synthesis of *Shigella flexneri* antigens [138]

docking analyzes, 7 positions (I228, A289, F290, I330, V331, D394, and R446) out of the 18 residues of the first shell of subsite +1 were judged to be critical for acceptor binding. They were systematically replaced by the 19 other possible residues, to generate a small library of 133 mutants of which several variants showed the required regioselectivity and stereoselectivity. The acceptor binding site of the enzyme was reshaped to enable the site-selective α-D-glucosylation of two non-natural acceptor monosaccharides, namely, methyl α-L-rhamnopyranoside and allyl 2-acetamido-2-deoxy-α-D-glucopyranoside [136, 137]. A product of enzymatic glucosylation—methyl α-D-glucopyranosyl-(1 → 3)-α-L-rhamnopyranoside—was further chemically elongated into a known building block compatible with chain extension at both sides to provide various fragments of the O-Ag from *S. flexneri* 3a, a prevalent serotype [135].

A more ambitious design relied on the engineering of several binding subsites of *Np*AS to render it able to glucosylate a partially protected disaccharide acceptor (allyl 2-deoxy-2-trichloroacetamido-β-D-glucopyranosyl-(1 → 2)-α-L-rhamnopyranoside) and generate a precursor of *S. flexneri*

1b O-antigen fragment [138]. An approach combining molecular docking, computational protein design, and information coming from amino acid conservation or pair correlation found in homologous enzymes was developed to design libraries containing a limited number of mutations at 23 selected positions of +1 and +2 subsites (Fig. 5). From the designed libraries of 63,000 clones selected from a set of 20^{23} theoretical combinations, one *Np*AS mutant was able to glucosylate the disaccharide of interest. A reaction for which there is no equivalent yet reported in the literature was made possible, generating the *S. flexneri* type 1b glucosylation pattern.

Following the same strategy, GH70 glucansucrases, *Np*AS, and GBD-CD2 branching sucrase were also tested in the glucosylation reaction of another lightly protected disaccharide acceptor: allyl α-L-rhamnopyranosyl-(1 → 2)-2-deoxy-2-trichloroacetamido-β-D-glucopyranoside, which is well suited for further chemical elongation leading to the *S. flexneri* type II glucosylation pattern. An incredibly high yield of site-selective α-D-glucosylation was obtained (80 %) without any additional engineering steps showing that screening natural diversity is worth being tried before starting any engineering work. Remarkably, the product of enzymatic glucosylation was chemically converted into the pentadecasaccharide hapten present in *S. flexneri* 2a-TT15, the first synthetic carbohydrate-based vaccine candidate against endemic shigellosis [139]. Whereas the overall yield of the chemo-enzymatic process does not necessarily compete with that of the chemical synthesis, these important achievements are strong cases to proceed forward.

One important fact to keep in mind is that once variant libraries are created for a specific purpose, they constitute a toolbox of catalysts diverging in specificity ready to be assayed with other unnatural substrates. A library of 171 single mutants targeting eight positions of subsite +1 and one position in subsite +2 of *Np*AS, which had been initially generated for rhamnoside and N-acetyl glucosamine glucosylation [135], was tested for luteolin glucosylation [140]. A preliminary molecular docking allowed checking that mutations in subsite +1 could also be beneficial for glucosylation of this flavonoid. Of 171 single mutants, 50 mutants synthesized luteolin glucosides with higher yield than the wild-type *Np*AS. Various profiles of glucosylation were obtained in which the relative amounts of mono-, di-, and tri-glucosylated luteolin varied. With mutant I228A of *Np*AS, 60 % of 5-mM luteolin was converted into glucosides versus 7 % for the parent enzyme. Further optimization allowed conversion of 72 % of 19-mM luteolin (4 g/L) to luteolin-4′-*O*-α-D-glucopyranoside and two di- and tri- glucosides, whose structures were never previously reported. These compounds were 2280-fold and 17,000-fold more water soluble than luteolin, respectively, showing that polyglucosylation profoundly modifies luteolin hydrophobic-lipophilic balance. UV absorption spectra of the various glucosides were similar to luteolin spectrum, and glycosylation was shown to protect the flavonoid against oxidation. All these results highlight the power of enzyme engineering to expand flavonoid glycoside libraries and promote investigations of their physicochemical and biological properties.

Conclusion/perspectives

Even though numerous data on amylosucrases and branching sucrases are available, biochemical characterization of these enzymes has remained limited to nine amylosucrases and five branching sucrases, and the 3D structure of only four of them has been determined. The available genomic data reveal that amylosucrases are much more widespread in the microbial world than branching sucrases, which have only been found in lactic acid bacteria to date. In the near future, biochemical characterization of a larger number of putative amylosucrases and branching sucrases should provide a wealth of data that will help us to understand their evolution, physiological role, and structure–activity relations.

The characterization of the branching sucrase particularities as compared with glucansucrases should also be a priority. In this view, replacement of amino acids conserved only in the branching enzymes by those conserved in glucansucrases through multiple-site mutagenesis should allow a better insight into the structural features that distinguish branching sucrases from glucansucrases. Structural comparison of the α-1,2 branching sucrase ΔN123 GBD-CD2 with glucansucrases also revealed significant differences in several loops of the $(\beta/\alpha)_8$ barrel. Structurally guided loop exchange could also be envisaged to investigate their roles in branching specificity. However, in the absence of crystal structures of enzyme complexes with long oligosaccharides bound in the active site, these approaches are drastically limited. Efforts must be pursued to obtain X-ray information from complexes and map the acceptor binding subsites to establish a more rational experimental design of mutagenesis experiments. Another important issue concerns the mode of branching. Do these enzymes release dextran (distributive mode) or retain dextran (processive mode) between two separate branching events? The α-1,2 branching enzyme ΔN123 GBD-CD2 was shown to be distributive to catalyze the glucosylation of oligosaccharides, and proposed to be semi-processive in the presence of high molar mass dextrans [100]. With the α-1,3 branching enzyme BRS-B, no experiment has been performed yet to investigate the processivity. However, acceptor reaction with BRS-B can yield branched dextrans containing up to 50 % α-1,3 linkages, with the implication

that every single glucosyl unit of the main chain is branched. It is tempting to suggest that a certain degree of processivity could take place and that the polymer chains are not released during branching. In such a scenario, domain V could be a key partner. Designing a set of experiments allowing these questions to be answered is essential to better control the incorporation of branching in the dextran acceptor.

Finally, the most challenging task to further elucidate enzymatic mechanisms is to tackle the question of the molecular dynamics of these catalysts. To date, it is impossible to have a full representation at the molecular level of the succession of events occurring at each enzyme cycle. Sucrose binding, fructose release, acceptor binding and glucosylation, and release of glucosylated product may be accompanied by conformational changes, as strongly suspected for both amylosucrases and branching sucrases. Tracking these conformational changes should also be a priority, altogether this should help to bridge structural and functional data and clarify, for example, the role of the secondary sugar binding sites SB2 and OB2 of *Np*AS, or that of the multiple sugar binding pockets at the surface of ΔN123 GBD-CD2 domain V. Furthermore, advances in these issues are essential to further develop knowledge-based methodologies of enzyme engineering and to incorporate this information into computer-based enzyme engineering strategies. This should improve the accuracy of the models, and accelerate reshaping of multiple binding sites to further expand the use of these enzymes for glycodiversification purposes.

Acknowledgments This work was supported by the French National Research Agency (ANR Project ENGEL; ANR-12CDII-0005). The authors thank the ICEO facility dedicated to enzyme screening and discovery, and part of the Integrated Screening Platform of Toulouse (PICT, IBiSA) for providing access to their equipments.

References

1. Leemhuis H, Pijning T, Dobruchowska JM et al (2013) Glucansucrases: three-dimensional structures, reactions, mechanism, α-glucan analysis and their implications in biotechnology and food applications. J Biotechnol 163:250–272
2. André I, Potocki-Véronèse G, Morel S et al (2010) Sucrose-utilizing transglucosidases for biocatalysis. In: Rauter AP, Vogel P, Queneau Y (eds) Carbohydrates sustainable development I. Springer, Berlin Heidelberg, pp 25–48
3. Cantarel BL, Coutinho PM, Rancurel C et al (2009) The Carbohydrate-Active EnZymes database (CAZy): an expert resource for glycogenomics. Nucleic Acids Res 37:D233–D238
4. Lombard V, Golaconda Ramulu H, Drula E et al (2014) The carbohydrate-active enzymes database (CAZy) in 2013. Nucleic Acids Res 42:D490–D495
5. Monsan P, Remaud-Siméon M, André I (2010) Transglucosidases as efficient tools for oligosaccharide and glucoconjugate synthesis. Curr Opin Microbiol 13:293–300
6. Daudé D, André I, Monsan P, Remaud-Simeon M (2014) Successes in engineering glucansucrases to enhance glycodiversification. In: Pilar Rauter A, Lindhorst T, Queneau Y (eds) Carbohydrate chemistry. Royal Society of Chemistry, Cambridge, pp 624–645
7. Hehre EJ, Hamilton DM (1946) Bacterial synthesis of an amylopectin-like polysaccharide from sucrose. J Biol Chem 51:777–778
8. Hehre EJ, Hamilton DM (1948) The conversion of sucrose to a polysaccharide of the starch-glycogen class by *Neisseria* from the pharynx. J Bacteriol 55:197–208
9. Hehre EJ (1949) Synthesis of a polysaccharide of the starch-glycogen class from sucrose by a cell-free, bacterial enzyme system (amylosucrase). J Biol Chem 177:267–279
10. MacKenzie CR, McDonald IJ, Johnson KG (1978) Glycogen metabolism in the genus Neisseria: synthesis from sucrose by amylosucrase. Can J Microbiol 24:357–362
11. Parker RB, Creamer HR (1971) Contribution of plaque polysaccharides to growth of cariogenic microorganisms. Arch Oral Biol 16:855–862
12. Ruby JD, Shirey RE, Gerencser VF, Stelzig DA (1982) Extracellular iodophilic polysaccharide synthesized by *Neisseria* in human dental plaque. J Dent Res 61:627–631
13. Riou JY, Guibourdenche M, Popoff MY (1983) A new taxon in the genus *Neisseria*. Ann Inst Pasteur Microbiol 134:257–267
14. Potocki de Montalk G, Remaud-Simeon M, Willemot RM, Planchot V, Monsan P (1999) Sequence analysis of the gene encoding amylosucrase from *Neisseria polysaccharea* and characterization of the recombinant enzyme. J Bacteriol 181:375–381
15. Potocki de Montalk G, Remaud-Simeon M, Willemot R-M et al (2000) Amylosucrase from *Neisseria polysaccharea:* novel catalytic properties. FEBS Lett 471:219–223
16. Schneider J, Fricke C, Overwin H, Hofer B (2011) High level expression of a recombinant amylosucrase gene and selected properties of the enzyme. Appl Microbiol Biotechnol 89:1821–1829
17. Pizzut-Serin S, Potocki-Véronèse G, van der Veen BA et al (2005) Characterisation of a novel amylosucrase from *Deinococcus radiodurans*. FEBS Lett 579:1405–1410
18. Emond S, Mondeil S, Jaziri K et al (2008) Cloning, purification and characterization of a thermostable amylosucrase from *Deinococcus geothermalis*. FEMS Microbiol Lett 285:25–32
19. Kim Myo-Deok, Seo Dong-Ho, Jung Jong-Hyun et al (2014) Molecular cloning and expression of amylosucrase from highly radiation-resistant *Deinococcus radiopugnans*. Food Sci Biotechnol 23:2007–2012
20. Seo D-H, Jung J-H, Choi H-C et al (2012) Functional expression of amylosucrase, a glucan-synthesizing enzyme, from A*rthrobacter chlorophenolicus* A6. J Microbiol Biotechnol 22:1253–1257
21. Ha S-J, Seo D-H, Jung J-H et al (2009) Molecular cloning and functional expression of a new amylosucrase from *Alteromonas macleodii*. Biosci Biotechnol Biochem 73:1505–1512
22. Jeong J-W, Seo D-H, Jung J-H et al (2014) Biosynthesis of glucosyl glycerol, a compatible solute, using intermolecular transglycosylation activity of amylosucrase from *Methylobacillus flagellatus* KT. Appl Biochem Biotechnol 173:904–917
23. Perez-Cenci M, Salerno GL (2014) Functional characterization of *Synechococcus* amylosucrase and fructokinase encoding genes discovers two novel actors on the stage of cyanobacterial sucrose metabolism. Plant Sci 224:95–102
24. But SY, Khmelenina VN, Reshetnikov AS et al (2015) Sucrose metabolism in halotolerant methanotroph *Methylomicrobium alcaliphilum* 20Z. Arch Microbiol 197:471–480
25. Buttcher V, Welsh T, Willmitzer L, Kossman J (1997) Cloning and characterization of the gene for amylosucrase from *Neisseria polysaccharea*: production of a linear alpha-1,4-glucan. J Bacteriol 179:3324–3330
26. Potocki de Montalk G, Remaud-Simeon M, Willemot R-M, Monsan P (2000) Characterisation of the activator effect of glycogen on amylosucrase from *Neisseria polysaccharea*. FEMS Microbiol Lett 186:103–108

27. Albenne C, Skov LK, Mirza O et al (2004) Molecular basis of the amylose-like polymer formation catalyzed by *Neisseria polysaccharea* amylosucrase. J Biol Chem 279:726–734
28. Khmelenina VN, Kalyuzhnaya MG, Sakharovsky VG et al (1999) Osmoadaptation in halophilic and alkaliphilic methanotrophs. Arch Microbiol 172:321–329
29. Hehre EJ (1941) Production from sucrose of A-serologically reactive polysaccharide by a sterile bacterial extract. Science 93:237–238
30. Jeanes A, Haynes WC, Wilham CA et al (1954) Characterization and classification of dextrans from ninety-six strains of bacteria. J Am Chem Soc 76:5041–5052
31. Seymour FR, Slodki ME, Plattner RD, Jeanes A (1977) Six unusual dextrans: methylation structural analysis by combined GCL-MS of per-*O*-acetyl-aldononitriles. Carbohydr Res 53:153–166
32. Mitsuishi Y, Kobayashi M, Matsuda K (1984) Structures of three α-D-(1 → 2)-branched oligosaccharides isolated from *Leuconostoc mesenteroides* NRRL B-1299 dextran. Carbohydr Res 127:331–337
33. Kobayashi M, Mitsuishi Y, Takagi S, Matsuda K (1984) Enzymic degradation of water-soluble dextran from *Leuconostoc mesenteroides* NRRL B-1299. Carbohydr Res 127:305–317
34. Seymour FR, Knapp RD (1980) Structural analysis of α-D-glucans by ^{13}C-nuclear magnetic resonance, spin-lattice relaxation studies. Carbohydr Res 81:67–103
35. Brooker BE (1976) Surface coat transformation and capsule formation by *Leuconostoc mesenteroides* NCDO 523 in the presence of sucrose. Arch Microbiol 111:99–104
36. Brooker BE (1977) Ultrastructural surface changes associated with dextran synthesis by *Leuconostoc mesenteroides*. J Bacteriol 131:288–292
37. Smith EE (1970) Biosynthetic relation between the soluble and insoluble dextrans produced by *Leuconostoc mesenteroides* NRRL B-1299. FEBS Lett 12:33–37
38. Dols M, Remaud-Simeon M, Monsan PF (1997) Dextransucrase production by *Leuconostoc mesenteroides* NRRL B-1299. Comparison with *L. mesenteroides* NRRL B-512F. Enzyme Microb Technol 20:523–530
39. Dols M, Remaud-Simeon M, Willemot RM et al (1998) Characterization of the different dextransucrase activities excreted in glucose, fructose, or sucrose medium by *Leuconostoc mesenteroides* NRRL B-1299. Appl Environ Microbiol 64:1298–1302
40. Bounaix M-S, Gabriel V, Morel S et al (2009) Biodiversity of exopolysaccharides produced from sucrose by sourdough lactic acid bacteria. J Agric Food Chem 57:10889–10897
41. Bounaix M-S, Gabriel V, Robert H et al (2010) Characterization of glucan-producing *Leuconostoc* strains isolated from sourdough. Int J Food Microbiol 144:1–9
42. Robert H, Gabriel V, Fontagné-Faucher C (2009) Biodiversity of lactic acid bacteria in French wheat sourdough as determined by molecular characterization using species-specific PCR. Int J Food Microbiol 135:53–59
43. Monchois V, Willemot R-M, Remaud-Simeon M et al (1996) Cloning and sequencing of a gene coding for a novel dextransucrase from *Leuconostoc mesenteroides* NRRL B-1299 synthesizing only α(1–6) and α(1–3) linkages. Gene 182:23–32
44. Monchois V, Remaud-Simeon M, Monsan P et al (1998) Cloning and sequencing of a gene coding for an extracellular dextransucrase (DSRB) from *Leuconostoc mesenteroides* NRRL B-1299 synthesizing only a α(1–6) glucan. FEMS Microbiol Lett 159:307–315
45. Bozonnet S, Dols-Laffargue M, Fabre E et al (2002) Molecular characterization of DSR-E, an α-1,2 linkage-synthesizing dextransucrase with two catalytic domains. J Bacteriol 184:5753–5761
46. Fabre E, Bozonnet S, Arcache A et al (2005) Role of the two catalytic domains of DSR-E dextransucrase and their involvement in the formation of highly α-1,2 branched dextran. J Bacteriol 187:296–303
47. Kang H-K, Nguyen TTH, Jeong H-N et al (2014) Molecular cloning and characterization of a novel glucansucrase from *Leuconostoc mesenteroides* subsp. mesenteroides LM34. Biotechnol Bioprocess Eng 19:605–612
48. Brison Y, Fabre E, Moulis C et al (2010) Synthesis of dextrans with controlled amounts of α-1,2 linkages using the transglucosidase GBD–CD2. Appl Microbiol Biotechnol 86:545–554
49. Brison Y, Pijning T, Malbert Y et al (2012) Functional and structural characterization of α-(1 → 2) branching sucrase derived from DSR-E glucansucrase. J Biol Chem 287:7915–7924
50. Passerini D, Vuillemin M, Laguerre S et al (2014) Complete Genome Sequence of *Leuconostoc citreum* Strain NRRL B-742. Genome Announc 2:e01179-14
51. Passerini D, Vuillemin M, Ufarté L et al (2015) Inventory of the GH70 enzymes encoded by *Leuconostoc citreum* NRRL B-1299—identification of three novel α-transglucosylases. FEBS J 282:2115–2130
52. Laguerre S, Amari M, Vuillemin M et al (2012) Genome sequences of three *Leuconostoc citreum* strains, LBAE C10, LBAE C11, and LBAE E16, isolated from wheat sourdoughs. J Bacteriol 194:1610–1611
53. Amari M, Valerie G, Robert H et al (2015) Overview of the glucansucrase equipment of *Leuconostoc citreum* LBAE-E16 and LBAE-C11, two strains isolated from sourdough. FEMS Microbiol Lett 362:1–8
54. Jeans A, Seymour FR (1979) The α-d-glucopyranosidic linkages of dextrans: comparison of percentages from structural analysis by periodate oxidation and by methylation. Carbohydr Res 74:31–40
55. Côté GL, Robyt JF (1983) The formation of α-D-(1 → 3) branch linkages by an exocellular glucansucrase from *Leuconostoc mesenteroides* NRRL B-742. Carbohydr Res 119:141–156
56. Remaud M, Paul F, Monsan P et al (1992) Characterization of α-(1 → 3) branched oligosaccharides synthesized by acceptor reaction with the extracellular glucosyltransferases from *L. mesenteroides* NRRL B-742. J Carbohydr Chem 11:359–378
57. Remaud-Simeon M, Vuillemin M, Moulis C et al. (2014) Polypeptide having the capacity to form alpha-1,3 glucosyl unit branchings on an acceptor. Patent WO 2014202208 A1
58. Stam MR, Danchin EGJ, Rancurel C et al (2006) Dividing the large glycoside hydrolase family 13 into subfamilies: towards improved functional annotations of α-amylase-related proteins. Protein Eng Des Sel 19:555–562
59. Jespersen HM, MacGregor EA, Henrissat B et al (1993) Starch- and glycogen-debranching and branching enzymes: prediction of structural features of the catalytic (β/α)8-barrel domain and evolutionary relationship to other amylolytic enzymes. J Protein Chem 12:791–805
60. Sarçabal P, Remaud-Simeon M, Willemot R-M et al (2000) Identification of key amino acid residues in *Neisseria polysaccharea* amylosucrase. FEBS Lett 474:33–37
61. Davies GJ, Wilson KS, Henrissat B (1997) Nomenclature for sugar-binding subsites in glycosyl hydrolases. Biochem J 321:557–559
62. Ferretti JJ, Gilpin ML, Russell RR (1987) Nucleotide sequence of a glucosyltransferase gene from *Streptococcus sobrinus* MFe28. J Bacteriol 169:4271–4278
63. Mooser G, Hefta SA, Paxton RJ et al (1991) Isolation and sequence of an active-site peptide containing a catalytic aspartic acid from two *Streptococcus sobrinus* alpha-glucosyltransferases. J Biol Chem 266:8916–8922

64. MacGregor EA, Jespersen HM, Svensson B (1996) A circularly permuted α-amylase-type α/β-barrel structure in glucan-synthesizing glucosyltransferases. FEBS Lett 378:263–266
65. Vujicic-Zagar A, Pijning T, Kralj S et al (2010) Crystal structure of a 117 kDa glucansucrase fragment provides insight into evolution and product specificity of GH70 enzymes. Proc Natl Acad Sci 107:21406–21411
66. Ito K, Ito S, Shimamura T et al (2011) Crystal structure of glucansucrase from the dental caries pathogen *Streptococcus mutans*. J Mol Biol 408:177–186
67. Skov LK, Mirza O, Henriksen A et al (2001) Amylosucrase, a glucan-synthesizing enzyme from the alpha-amylase family. J Biol Chem 276:25273–25278
68. Mirza O, Skov LK, Remaud-Simeon M et al (2001) Crystal structures of amylosucrase from *Neisseria polysaccharea* in complex with D-glucose and the active site mutant Glu328Gln in complex with the natural substrate sucrose. Biochemistry 40:9032–9039
69. Skov LK, Mirza O, Sprogøe D et al (2002) Oligosaccharide and sucrose complexes of amylosucrase. Structural implications for the polymerase activity. J Biol Chem 277:47741–47747
70. Jensen MH, Mirza O, Albenne C et al (2004) Crystal structure of the covalent intermediate of amylosucrase from *Neisseria polysaccharea*. Biochemistry 43:3104–3110
71. Guerin F, Barbe S, Pizzut-Serin S et al (2012) Structural investigation of the thermostability and product specificity of amylosucrase from the bacterium *Deinococcus geothermalis*. J Biol Chem 287:6642–6654
72. Skov LK, Pizzut-Serin S, Remaud-Simeon M et al (2013) The structure of amylosucrase from *Deinococcus radiodurans* has an unusual open active-site topology. Acta Crystallograph Sect F Struct Biol Cryst Commun 69:973–978
73. Albenne C, Skov LK, Tran V et al (2006) Towards the molecular understanding of glycogen elongation by amylosucrase. Proteins Struct Funct Bioinform 66:118–126
74. Cambon E, Barbe S, Pizzut-Serin S et al (2014) Essential role of amino acid position 226 in oligosaccharide elongation by amylosucrase from *Neisseria polysaccharea*: amylosucrase engineering for high amylose production. Biotechnol Bioeng 111:1719–1728
75. Pijning T, Vujičić-Žagar A, Kralj S et al (2012) Structure of the α-1,6/α-1,4-specific glucansucrase GTFA from *Lactobacillus reuteri* 121. Acta Crystallograph Sect F Struct Biol Cryst Commun 68:1448–1454
76. Uitdehaag J, Mosi R, Kalk K et al (1999) X-ray structures along the reaction pathway of cyclodextrin glycosyltransferase elucidate catalysis in the α-amylase family. Nat Struct Biol 6:432–436
77. Mooser G, Wong C (1988) Isolation of a glucan-binding domain of glucosyltransferase (1,6-alpha-glucan synthase) from *Streptococcus sobrinus*. Infect Immun 56:880–884
78. Banas JA, Russell RR, Ferretti JJ (1990) Sequence analysis of the gene for the glucan-binding protein of *Streptococcus mutans* Ingbritt. Infect Immun 58:667–673
79. Gilmore KS, Russell RR, Ferretti JJ (1990) Analysis of the *Streptococcus downei* gtfS gene, which specifies a glucosyltransferase that synthesizes soluble glucans. Infect Immun 58:2452–2458
80. Abo H, Matsumura T, Kodama T et al (1991) Peptide sequences for sucrose splitting and glucan binding within *Streptococcus sobrinus* glucosyltransferase (water-insoluble glucan synthetase). J Bacteriol 173:989–996
81. Giffard PM, Simpson CL, Milward CP, Jacques NA (1991) Molecular characterization of a cluster of at least two glucosyltransferase genes in *Streptococcus salivarius* ATCC 25975. J Gen Microbiol 137:2577–2593
82. Giffard PM, Allen DM, Milward CP et al (1993) Sequence of the gtfK gene of *Streptococcus salivarius* ATCC 25975 and evolution of the gtf genes of oral streptococci. J Gen Microbiol 139:1511–1522
83. Giffard PM, Jacques NA (1994) Definition of a fundamental repeating unit in streptococcal glucosyltransferase glucan-binding regions and related sequences. J Dent Res 73:1133–1141
84. Komatsu H, Katayama M, Sawada M et al (2007) Thermodynamics of the binding of the C-terminal repeat domain of *Streptococcus sobrinus* glucosyltransferase-I to dextran. Biochemistry 46:8436–8444
85. Suwannarangsee S, Moulis C, Potocki-Veronese G et al (2007) Search for a dextransucrase minimal motif involved in dextran binding. FEBS Lett 581:4675–4680
86. Mori T, Asakura M, Okahata Y (2011) Single-molecule force spectroscopy for studying kinetics of enzymatic dextran elongations. J Am Chem Soc 133:5701–5703
87. Kingston KB, Allen DM, Jacques NA (2002) Role of the C-terminal YG repeats of the primer-dependent streptococcal glucosyltransferase, GtfJ, in binding to dextran and mutan. Microbiol 148:549–558
88. Pijning T, Vujičić-Žagar A, Kralj S et al (2014) Flexibility of truncated and full-length glucansucrase GTF180 enzymes from *Lactobacillus reuteri* 180. FEBS J 281:2159–2171
89. Wang R, Bae J-S, Kim J-H et al (2012) Development of an efficient bioprocess for turanose production by sucrose isomerisation reaction of amylosucrase. Food Chem 132:773–779
90. Potocki-Veronese G, Putaux J-L, Dupeyre D et al (2005) Amylose synthesized in vitro by amylosucrase: morphology, structure, and properties. Biomacromolecules 6:1000–1011
91. Roblin P, Potocki-Véronèse G, Guieysse D et al (2013) SAXS conformational tracking of amylose synthesized by amylosucrases. Biomacromolecules 14:232–239
92. Grimaud F, Lancelon-Pin C, Rolland-Sabaté A et al (2013) In vitro synthesis of hyperbranched α-glucans using a biomimetic enzymatic toolbox. Biomacromolecules 14:438–447
93. Rolland-Sabaté A, Guilois S, Grimaud F et al (2014) Characterization of hyperbranched glycopolymers produced in vitro using enzymes. Anal Bioanal Chem 406:1607–1618
94. Kim H-H, Jung J-H, Seo D-H et al (2011) Novel enzymatic production of trehalose from sucrose using amylosucrase and maltooligosyltrehalose synthase-trehalohydrolase. World J Microbiol Biotechnol 27:2851–2856
95. Schneider J, Fricke C, Overwin H et al (2009) Generation of amylosucrase variants that terminate catalysis of acceptor elongation at the di- or trisaccharide stage. Appl Environ Microbiol 75:7453–7460
96. Putaux J-L, Potocki-Véronèse G, Remaud-Simeon M, Buleon A (2006) α-D-Glucan-based dendritic nanoparticles prepared by in vitro enzymatic chain extension of glycogen. Biomacromolecules 7:1720–1728
97. Rolland-Sabaté A, Colonna P, Potocki-Véronèse G et al (2004) Elongation and insolubilisation of α-glucans by the action of *Neisseria polysaccharea* amylosucrase. J Cereal Sci 40:17–30
98. Kim BK, Kim HI, Moon TW, Choi SJ (2014) Branch chain elongation by amylosucrase: production of waxy corn starch with a slow digestion property. Food Chem 152:113–120
99. Kim B-S, Kim H-S, Hong J-S et al (2013) Effects of amylosucrase treatment on molecular structure and digestion resistance of pregelatinised rice and barley starches. Food Chem 138:966–975
100. Brison Y, Laguerre S, Lefoulon F et al (2013) Branching pattern of gluco-oligosaccharides and 1.5 kDa dextran grafted by the α-1,2 branching sucrase GBD-CD2. Carbohydr Polym 94:567–576
101. Sarbini SR, Kolida S, Naeye T et al (2011) In vitro fermentation of linear and -1,2-branched dextrans by the human fecal microbiota. Appl Environ Microbiol 77:5307–5315
102. Djouzi Z, Andrieux C, Pelenc V et al (1995) Degradation and fermentation of α-gluco-oligosaccharides by bacterial strains

from human colon: in vitro and in vivo studies in gnotobiotic rats. J Appl Bacteriol 79:117–127
103. Valette P, Pelenc V, Djouzi Z et al (1993) Bioavailability of new synthesised glucooligosaccharides in the intestinal tract of gnotobiotic rats. J Sci Food Agric 62:121–127
104. Serino M, Luche E, Gres S et al (2012) Metabolic adaptation to a high-fat diet is associated with a change in the gut microbiota. Gut 61:543–553
105. Serino M, Cenac C, Chabo C et al (2009) O57 Spécificité métagénomique de la flore intestinale, perméabilité intestinale, et métabolisme chez des souris diabétiques. Effets réversibles par les glucooligosaccharides. Diabetes Metab 35:A15
106. Daudé D, Champion E, Morel S et al (2013) Probing substrate promiscuity of amylosucrase from *Neisseria polysaccharea*. Chem Cat Chem 5:2288–2295
107. Lee B-H, Koh D-W, Territo PR et al (2015) Enzymatic synthesis of 2-deoxyglucose-containing maltooligosaccharides for tracing the location of glucose absorption from starch digestion. Carbohydr Polym 132:41–49
108. Park H (2012) Bioconversion of piceid to piceid glucoside using amylosucrase from *Alteromonas macleodii* Deep Ecotype. J Microbiol Biotechnol 22:1698–1704
109. Quideau S, Deffieux D, Douat-Casassus C, Pouységu L (2011) Plant polyphenols: chemical properties, biological activities, and synthesis. Angew Chem Int Ed 50:586–621
110. Del Rio D, Rodriguez-Mateos A, Spencer JPE et al (2013) Dietary (Poly)phenolics in human health: structures, bioavailability, and evidence of protective effects against chronic diseases. Antioxid Redox Signal 18:1818–1892
111. Plaza M, Pozzo T, Liu J et al (2014) Substituent effects on in vitro antioxidizing properties, stability, and solubility in flavonoids. J Agric Food Chem 62:3321–3333
112. De Martino L, Mencherini T, Mancini E et al (2012) In vitro phytotoxicity and antioxidant activity of selected flavonoids. Int J Mol Sci 13:5406–5419
113. Palcic MM (2011) Glycosyltransferases as biocatalysts. Curr Opin Chem Biol 15:226–233
114. Desmet T, Soetaert W, Bojarová P et al (2012) Enzymatic glycosylation of small molecules: challenging substrates require tailored catalysts. Chem Eur J 18:10786–10801
115. Nakahara K, Kontani M, Ono H et al (1995) Glucosyltransferase from *Streptococcus sobrinus* catalyzes glucosylation of catechin. Appl Environ Microbiol 61:2768–2770
116. Meulenbeld GH, Zuilhof H, van Veldhuizen A et al (1999) Enhanced (+)-catechin transglucosylating activity of *Streptococcus mutans* GS-5 glucosyltransferase-D due to fructose removal. Appl Environ Microbiol 65:4141–4147
117. Meulenbeld GH, Hartmans S (2000) Transglycosylation by *Streptococcus mutans* GS-5 glucosyltransferase-D: acceptor specificity and engineering of reaction conditions. Biotechnol Bioeng 70:363–369
118. Bertrand A, Morel S, Lefoulon F et al (2006) *Leuconostoc mesenteroides* glucansucrase synthesis of flavonoid glucosides by acceptor reactions in aqueous-organic solvents. Carbohydr Res 341:855–863
119. Moon Y-H, Lee J-H, Jhon D-Y et al (2007) Synthesis and characterization of novel quercetin-α-D-glucopyranosides using glucansucrase from *Leuconostoc mesenteroides*. Enzyme Microb Technol 40:1124–1129
120. Woo H-J, Kang H-K, Nguyen TTH et al (2012) Synthesis and characterization of ampelopsin glucosides using dextransucrase from *Leuconostoc mesenteroides* B-1299CB4: glucosylation enhancing physicochemical properties. Enzyme Microb Technol 51:311–318
121. Kim G-E, Kang H-K, Seo E-S et al (2012) Glucosylation of the flavonoid, astragalin by *Leuconostoc mesenteroides* B-512FMCM dextransucrase acceptor reactions and characterization of the products. Enzyme Microb Technol 50:50–56
122. Cho H-K, Kim H-H, Seo D-H et al (2011) Biosynthesis of (+)-catechin glycosides using recombinant amylosucrase from *Deinococcus geothermalis* DSM 11300. Enzyme Microb Technol 49:246–253
123. Seo D-H, Jung J-H, Ha S-J et al (2012) High-yield enzymatic bioconversion of hydroquinone to α-arbutin, a powerful skin lightening agent, by amylosucrase. Appl Microbiol Biotechnol 94:1189–1197
124. Seo D-H, Jung J-H, Lee J-E et al (2012) Biotechnological production of arbutins (α- and β-arbutins), skin-lightening agents, and their derivatives. Appl Microbiol Biotechnol 95:1417–1425
125. Kim KH, Park Y-D, Park H et al (2014) Synthesis and biological evaluation of a novel baicalein glycoside as an anti-inflammatory agent. Eur J Pharmacol 744:147–156
126. Overwin H, Wray V, Hofer B (2015) Biotransformation of phloretin by amylosucrase yields three novel dihydrochalcone glucosides. J Biotechnol 211:103–106
127. André I, Potocki-Véronèse G, Barbe S et al (2014) CAZyme discovery and design for sweet dreams. Curr Opin Chem Biol 19:17–24
128. Turner NJ, O'Reilly E (2013) Biocatalytic retrosynthesis. Nat Chem Biol 9:285–288
129. Bornscheuer UT, Huisman GW, Kazlauskas RJ et al (2012) Engineering the third wave of biocatalysis. Nature 485:185–194
130. Höhne M, Schätzle S, Jochens H et al (2010) Rational assignment of key motifs for function guides in silico enzyme identification. Nat Chem Biol 6:807–813
131. Kries H, Blomberg R, Hilvert D (2013) De novo enzymes by computational design. Curr Opin Chem Biol 17:221–228
132. Kiss G, Çelebi-Ölçüm N, Moretti R et al (2013) Computational enzyme design. Angew Chem Int Ed 52:5700–5725
133. Phalipon A, Mulard LA, Sansonetti PJ (2008) Vaccination against shigellosis: is it the path that is difficult or is it the difficult that is the path? Microbes Infect 10:1057–1062
134. Jennison AV, Verma NK (2004) *Shigella flexneri* infection: pathogenesis and vaccine development. FEMS Microbiol Rev 28(43–58):140
135. Champion E, André I, Moulis C et al (2009) Design of α-transglucosidases of controlled specificity for programmed chemoenzymatic synthesis of antigenic oligosaccharides. J Am Chem Soc 131:7379–7389
136. Champion E, Moulis C, Morel S et al (2010) A pH-based high-throughput screening of sucrose-utilizing transglucosidases for the development of enzymatic glucosylation tools. Chem Cat Chem 2:969–975
137. Champion E, Guérin F, Moulis C et al (2012) Applying pairwise combinations of amino acid mutations for sorting out highly efficient glucosylation tools for chemo-enzymatic synthesis of bacterial oligosaccharides. J Am Chem Soc 134:18677–18688
138. Verges A, Cambon E, Barbe S et al (2015) Computer-aided engineering of a transglycosylase for the glucosylation of an unnatural disaccharide of relevance for bacterial antigen synthesis. ACS Catal 5:1186–1198
139. Salamone S, Guerreiro C, Cambon E et al (2015) Programmed chemo-enzymatic synthesis of the oligosaccharide component of a carbohydrate-based antibacterial vaccine candidate. Chem Commun 51:2581–2584
140. Malbert Y, Pizzut-Serin S, Massou S et al (2014) Extending the structural diversity of α-flavonoid glycosides with engineered glucansucrases. Chem Cat Chem 6:2282–2291